KOGNITIVE NEUROPHYSIOLOGIE DES MENSCHEN

HUMAN COGNITIVE NEUROPHYSIOLOGY

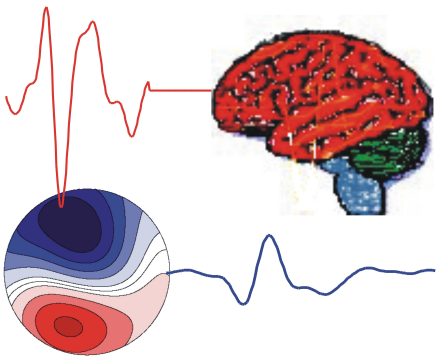

Impressum
Herausgeber: Wolfgang Skrandies

wolfgang.skrandies@physiologie.med.uni-giessen.de

ISSN 1867-576X

Kognitive Neurophysiologie des Menschen wurde im Jahr 2008 gegründet. Hier sollen wissenschaftliche Artikel zu Themen der kognitiven Neurophysiologie des Menschen erscheinen Sowohl Beiträge über Methoden als auch Ergebnisse der Grundlagen- und klinischen Forschung werden akzeptiert. Jedes Manuskript wird von 3 unabhängigen Gutachtern beurteilt und so rasch wie möglich publiziert werden.
Die Zeitschrift ist ein elektronisches "Open Access"-Journal, ohne kommerzielle Interessen; `http://geb.uni-giessen.de/geb/volltexte/2008/6504/.`
Eine dauerhafte Präsenz der Zeitschrift im Internet wird durch die Universität Giessen gewährleistet.

Human Cognitive Neurophysiology was founded in 2008. This journal will publish contributions on methodological advances as well as results from basic and applied research on cognitive neurophysiology. Both German and English manuscripts will be accepted. Each manuscript will be reviewed by three independent referees.
This is an electronic "Open Access"-Journal with no commercial interest, published at `http://geb.uni-giessen.de/geb/volltexte/2008/6504/.`
Online presence is guaranteed by the University of Giessen.

Instructions for Authors

Only original and unpublished work will be considered for publication unless it is explicitly stated that the topic is a review. All manuscripts will be peer-reviewed. Both German and English versions are acceptable. After publication, the copyright will be with the editor of the journal. Usage of published material for review papers will be granted. Manuscripts (as `WORD` or `TEX files`) should be sent to `wolfgang.skrandies@physiologie.med.uni-giessen.de.`

Organization of manuscripts: The title page with a concise title should give the authors' names, address(es), and e-mail address of the corresponding author. The manuscript should include an abstract in English (maximum 300 words). Organize your work in the sections Introduction, Methods, Results, Discussion, and Literature. Please also supply a short list of keywords that may help to find your publication.

Illustrations: All figures should be submitted as `jpeg` or `Coreldraw` files. Please supply figure legends that explain the content of the figures in detail. Since this is an electronic journal color figures will be published free-of-charge.

The *Literature* should only include papers that have been published or accepted for publication. The reference list should be in alphabetical order by author. In the text, references should be cited by author(s) and year (e.g. Johnson, Hsiao, & Twombly, 1995; Pascual-Marqui, Michel, & Lehmann, 1994; Zani & Proverbio, 2002).

Examples of reference format

Johnson, K., Hsiao, S., & Twombly, L. (1995). Neural mechanisms of tactile form recognition. In M. Gazzaniga (Ed.), *The Cognitive Neurosciences* (p. 253-267). Cambridge, Mass.: MIT Press.

Pascual-Marqui, R., Michel, C., & Lehmann, D. (1994). Low resolution electromagnetic tomography: a new method for localizing electrical activity in the brain. *International Journal of Psychophysiology*, *18*, 49-65.

Zani, A., & Proverbio, A. (Eds.). (2002). *The Cognitive Electrophysiology of Mind and Brain*. San Diego: Elsevier.

Inhalt — Contents

Abstract

M. Wagner, C. Ponton, R. Tech, M. Fuchs, & J. Kastner (Hamburg, Germany & Charlotte, USA)
Non-Parametric Statistical Analysis of EEG/MEG Map Topographies and Source Distributions on the Epoch Level

In Event-Related Potential and Event-Related Field experiments, stimuli – often of several different types – are presented repeatedly, and the subject's brain response is recorded using Electroencephalography (EEG) or, in the ERF case, Magnetoencephalography (MEG). After removing artifacts and epoching the data, many repetitions per stimulus type are available, which are later usually averaged and compared. At this stage, though, it is no longer possible to establish whether and for which latencies the averaged waveforms are significantly different between stimulus types, nor whether the epochs for a given stimulus type yield significant averages in the first place. A statistical analysis of all individual epochs can provide exactly this information. Topographic Analysis of Variance (TANOVA) and Statistical non-Parametric Mapping performed on the results of Current Density Reconstructions (CDR SnPM) are non-parametric permutation or randomization tests which have previously been published but mainly been used to process per-subject averaged EEG data in the context of group studies. This paper describes how to apply TANOVA and CDR SnPM to individual epochs on a sample-by-sample basis, even in the context of single-subject data. A multiple comparison correction approach for the analysis of subsequent samples based on spectral properties of the data is presented. Methods are demonstrated using filtered and unfiltered simulated dipole data and data from a Continuous Performance Task (CPT) EEG experiment eliciting Mismatch Negativity. While TANOVA is able to identify latencies of significantly different map topographies, CDR SnPM extracts – per latency – the locations of significant source activation differences between stimulus types, albeit at the price of reduced overall sensitivity. Using simulated data, the proposed multiple comparison correction approach is illustrated. Significant peaks and source locations obtained for the CPT data are consistent with existing knowledge.

Keywords: Electroencephalography, Magnetoencephalography, Event-Related Fields, Event-Related Potentials, Continuous Performance Task, Statistical Analysis, Randomization Statistics, Non-Parametrical Statistics, Topographical Analysis of Variance, Current Density Analysis, Statistical non-Parametric Mapping

M. Wagner, C. Ponton, R. Tech, M. Fuchs, & J. Kastner — Non-Parametric Statistical Analysis of EEG/MEG Map Topographies and Source Distributions on the Epoch Level

M. Wagner[1], C. Ponton[2], R. Tech[1], M. Fuchs[1], & J. Kastner[1]
[1]Compumedics Germany GmbH, Heußweg 25, 20255 Hamburg, Germany,
[2]Compumedics USA Inc., 6605 West WT Harris Blvd, Charlotte, NC 28269, USA
mwagner@neuroscan.com

Introduction

In an Event-Related Potential (ERP) or Event-Related Field (ERF) experiment, an Electroencephalography (EEG) or Magnetoencephalography (MEG) device records the brain response related to a sensory, cognitive, or motor event. Depending on the experimental design, events (stimuli or responses) may be of the same or of different types. Data segments with distortions such as ocular, cardiac, or muscle artifacts are later detected and artifacts are either reduced or excluded from further processing. After splitting the data into epochs time-locked to events, many repetitions per event type are available and usually averaged and compared. After averaging, though, it is no longer possible to establish whether and for which latencies the averaged waveforms differ significantly between event types, nor whether the trials (epochs) of a given type yield significant averages in the first place. A statistical analysis of all individual epochs can provide this information.

Traditional statistical measures in channel space such as the *t*-test make disputable assumptions regarding repeatability and independence (Murray, Brunet, & Michel, 2008; Koenig & Melie-García, 2009). Therefore, a new non-parametric family of methods has recently attracted attention as it became computationally feasible for the analysis of ERP group studies (Murray et al., 2004). Although – misleadingly – referred to as Topographic Analysis of Variance (TANOVA, Koenig & Melie-García, 2010), no analysis of variance is being conducted, but rather a non-parametric permutation or randomization test. TANOVA is usually applied to per-subject averaged data in the context of group studies and yields similarities within and differences between groups of subjects.

If distributed source analysis methods such as Current Density Reconstruction (CDR) are used to localize the neural generators, the additional question of where in the brain significantly different source topographies occur may be asked. Statistical non-Parametric Mapping (SnPM) by non-parametric permutation or randomization tests using a maximum statistic to control the Family-Wise Error Rate (FWER) provides an assumption-free environment to answer this question (Nichols & Holmes, 2002). In the context of EEG, CDR SnPM is typically applied to source analysis results obtained for averaged data in the context of group studies and used to assess differences between groups of subjects (J. S. Kim, Han, Park, & Chung, 2008; Y. Y. Kim et al., 2009).

In this contribution, a framework is described that allows the application of the existing methods TANOVA and SnPM not only to individual averages in the context of an ERP/ERF group

study but to the individual epochs themselves (Wagner, 2014), something that is even possible for single-subject data. Unlike described in previous publications, the statistical analysis is conducted sample-by-sample as opposed to using a maximum statistic over all samples (Pantazis, Nichols, Baillet, & Leahy, 2003; R. E. Greenblatt & Pflieger, 2004), thus following the approach presented by (Koenig & Melie-García, 2009) for group data, but using a multiple comparison correction that is based on the spectral properties of the data. For CDR SnPM, in addition to the test for significant differences between conditions, a within-condition consistency test is proposed which can be used to justify testing for differences on a sample-by-sample basis. Standardized Low Resolution Electromagnetic Tomography (sLORETA) in a realistically shaped head model is employed for source localization, because it yields low localization error for focal activity, uniform spatial sensitivity, and is robust with respect to regularization (Pascual-Marqui, 2002; Wagner, Fuchs, & Kastner, 2004).

A simulation study is used to validate the implementation, and a visual Continuous Performance Task (CPT) EEG experiment eliciting Mismatch Negativity (MMN) is used to demonstrate the methods. The following Methods section is ordered by data acquisition and processing steps. However, the simulation study is described last, as it builds upon methods described previously.

Methods

Visual Continuous Performance Task Experiment

The numbers "1" and "2" were used as visual stimuli. In a visual CPT paradigm, "1" was used as the target stimulus and "2" as the distractor stimulus. The subject, a healthy adult, had EEG electrodes attached while watching the presentation of stimuli on a computer screen. 31 EEG electrodes were placed according to an extended 10-20 system with additional *FPz, FCz, CPz, Oz, FC3/4, CP3/4, FT7/8,* and *TP7/8* contacts (Fig. 1). The stimulus duration was 200 ms, with a randomized inter-stimulus interval (ISI) of between 800 ms and 1300 ms. 41 target and 165 distractor stimuli were presented in randomized order using the STIM system (Compumedics, Charlotte, NC, USA). The subject was instructed to press a button following the presentation of each target stimulus. EEG and VEOG data were recorded using a 32-channel Neuroscan system (Compumedics, Charlotte, NC, USA) with a sampling frequency of 250 Hz and a high-pass filter of 0.15 Hz.

Signal processing was performed in the Curry 7 software (Compumedics, Charlotte, NC, USA). Data were re-referenced to a Common Average Reference (CAR), because the subsequently applied statistical and source analysis methods require CAR data, and filtered using a 40 Hz low-pass filter. Eye blink effects were reduced using a regression analysis in combination with artifact averaging (Semlitsch et al., 1986). Data were epoched from 200 ms before to 500 ms after stimulus onset (Fig. 1). Epochs with signals exceeding ± 30 µV were excluded, since a visual inspection of the common average referenced epochs showed that signals of this magnitude were likely due to artifact. Averages for both stimulus types were

computed (Fig. 2). In the following, this dataset will be referred to as the low-pass filtered CPT data. In order to explore the effects of filtering on the statistics outcome, data were alternatively processed and epoched without any additional filtering besides the 0.15 Hz data acquisition filter, and with a high-pass of 1 Hz, 2 Hz, and 3 Hz in addition to the 40 Hz low-pass. To investigate statistics outcome for reduced epoch counts, derived versions of the low-pass filtered CPT data with only 75 %, 50 %, and 25 % of the total number of epochs were created. These three new, decimated datasets were obtained by excluding every fourth or every second epoch, or retaining only every fourth epoch, respectively.

Topographic Analysis of Variance

In the context of a TANOVA, two different non-parametric randomization tests were performed for all epochs: a consistency test per event type, and a test for differences between event types. Both tests were already described in (Koenig & Melie-García, 2010) and are summarized here for reference only.

The consistency test evaluates field topography (map) similarity across epochs. It is performed independently for each event type and each sample. Here, the Null Hypothesis is that epochs of the same event type are unrelated, i.e. that random maps have been measured. If the Null Hypothesis holds, randomly perturbing channels within each epoch's maps should not deteriorate the average map across all epochs.

For each sample s and Ec epochs of event type c, the test is performed as follows: First, the observed mean global field power (MGFP) $P_{s,c,0}$ of the average over all epochs e of the individual maps $d_{s,c,e}$ is computed as

$$P_{s,c,0} = \mathrm{mgfp}\left(\frac{1}{E_c}\sum_{e=1}^{E_c} d_{s,c,e}\right) \qquad (1)$$

with

$$\mathrm{mgfp}(d) = \sqrt{\frac{1}{M}\sum_{i=1}^{M}\left(d_i - \frac{1}{M}\sum_{j=1}^{M} d_j\right)^2}$$

where M is the number of channels. Then, for a total of R repetitions, the channels within each map are randomly shuffled or perturbed. Typically, perturbation is used if the total number of perturbations is computationally feasible, while randomization is used in all other scenarios, including most real-world applications. For each repetition r, this yields new randomized maps $d_{s,c,e,r}$, and a new global field power $P_{s,c,r}$ can be computed according to

$$P_{s,c,r} = \mathrm{mgfp}\left(\frac{1}{E_c}\sum_{e=1}^{E_c} d_{s,c,e,r}\right). \qquad (2)$$

The probability $p_{s,c}$ of the Null Hypothesis is the fraction of values $P_{s,c,r}$ that are larger than or equal to $P_{s,c,0}$. Small values of p, traditionally $p < 0.05$, indicate rejection of the Null Hypothesis, or consistency between epochs of the same event type. The number of possible permutations is $M!$ (Nichols & Holmes, 2002) and must be larger than the number of randomizations, which is typically the case for 8 and more channels.

The test for differences between event types is again performed independently for each sample. Here, the Null Hypothesis is that there is no difference between event types, i.e. that the same maps occur regardless of event type. If the Null Hypothesis holds, randomly perturbing maps across event types should not alter the average maps per event type.

When just two event types are compared, the MGFP of the difference of the averaged maps per

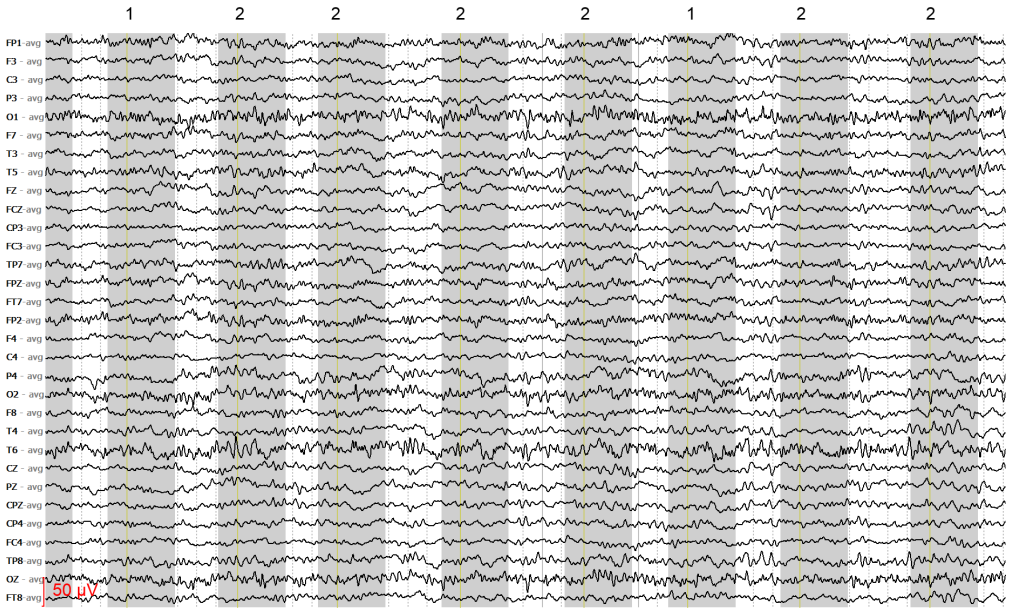

Figure 1: A 10 s page of ongoing EEG data re-referenced to CAR, with stimulus types at the top, where "1" stands for target and "2" represents distractor stimuli. Latency ranges marked in gray were used for epoching, from 200 ms pre- to 500 ms post-stimulus onset.

event type can serve as the measure. For each sample, the test is performed as follows: In a first step, the observed global field power $P_{s,0}$ of the difference of the averages over all epochs of event types $c = 1$ and $c = 2$ is computed as

$$P_{s,0} = \mathrm{mgfp}\left(\frac{1}{E_1}\sum_{e=1}^{E_1} d_{s,1,e} - \frac{1}{E_2}\sum_{e=1}^{E_2} d_{s,2,e}\right). \quad (3)$$

For R repetitions, maps are then randomly shuffled across event types. For each repetition r, randomized maps $d_{s,c,e,r}$ are obtained and the global field power $P_{s,r}$ can be computed according to

$$P_{s,r} = \mathrm{mgfp}\left(\frac{1}{E_1}\sum_{e=1}^{E_1} d_{s,1,e,r} - \frac{1}{E_2}\sum_{e=1}^{E_2} d_{s,2,e,r}\right). \quad (4)$$

Again, the probability p_s of the Null Hypothesis is the fraction of values $P_{s,r}$ that are larger than or equal to $P_{s,0}$. Small values of p indicate significant map differences between event types. Because an omnibus measure of map similarity has been used, no correction for multiple testing is necessary. The number of possible permutations, which again must be larger than the number of randomizations, is $(E_1+E_2)!/E_1!\cdot E_2!$ (Nichols & Holmes, 2002), which is typically the case for 8 and more epochs per type.

As both the consistency test and the difference test are performed sample by sample, false positives are to be expected. A test for the significance of consecutive rejections of the Null Hypothesis can establish, whether such periods of significance are significant themselves and is described in Koenig and Melie-García (2009).

Optionally, data may be collapsed across samples of interest to increase the Signal-to-Noise Ratio (SNR). Averaged maps may be normalized before computing the difference, in order to ignore absolute effect sizes. An extension to more

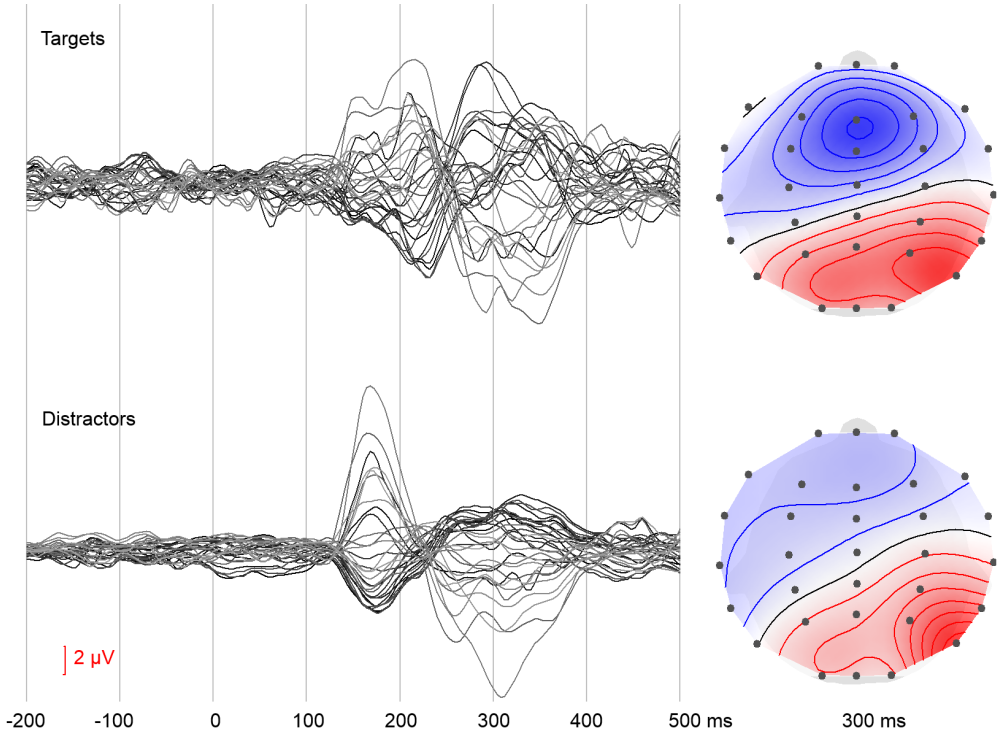

Figure 2: Butterfly plots of the average waveforms (left) and voltage topography maps for the 300 ms latency (right) for both stimulus types.

than two and to different categories of event types using a measure called global dissimilarity is described in Murray et al. (2008). TANOVA computation times scale linearly with the number of samples, number of randomizations, and number of channels.

TANOVA analysis was performed using the Curry software. For this paper, values of $p < 0.05$ were regarded as significant. As suggested by Manly (2006), the corresponding required number of repetitions was chosen to be $R = 50/p = 1000$. Map normalization was used for the difference tests, such that the MGFP per map was equal to 1. The complete time range from -200 ms to 500 ms was analyzed for the differently filtered and decimated data sets.

Source Analysis

A standardized Low Resolution Electromagnetic Tomography (sLORETA) analysis (Pascual-Marqui, 2002; Wagner et al., 2004) was performed for each sample of every epoch. As the head model, a realistically shaped three-compartment Boundary Element Method (BEM) model comprising 8043 nodes and 16074 triangles was used (Fuchs, Wagner, & Kastner, 2001). Conductivities were assumed to be 0.33, 0.0132, and 0.33 S/m for the skin, skull, and brain compartment, respectively. Source locations were distributed on a 7 mm regular grid throughout the brain but excluding the cerebellum, yielding a total of $N = 4786$ locations. The regularization parameter was determined

according to the discrepancy principle (Fuchs, Wagner, Köhler, & Wischmann, 1999) using an sLORETA analysis of the grand average of all epochs and subsequently kept fixed throughout the individual epoch analyses.

For the remainder of this paper, the resulting source strength distribution for sample s, event type c, and epoch e will be referred to as a source image $I_{s,c,e}$ and each source location will be referred to as a voxel n, with $i_{s,c,e,n}$ the source intensity at that particular voxel. In spite of this notation, the concept of a voxel readily generalizes to cases where sources are computed on the folded cortical surface only (Wagner, Fuchs, Wischmann, Ottenberg, & Dössel, 1995).

Statistical non-Parametric Mapping

The input data for SnPM can be CDR source images, but also beamformer results or voltage topographies (R. E. Greenblatt & Pflieger, 2004). In this case, sLORETA source images are used, which have the property to be normalized to the standard deviation per voxel (Pascual-Marqui, 2002). As a consequence, using sLORETA images as input data for SnPM yields uniform spatial sensitivity of the statistical test (Pantazis et al., 2003). As for TANOVA, a consistency test per event type and a test for differences between event types can be performed.

The consistency test evaluates source image similarity across epochs. It is performed independently for each event type and each sample. Here, the Null Hypothesis is that epochs of the same event type are unrelated, i.e. that random source images have been computed. If the Null Hypothesis holds, randomly perturbing voxels within each epoch's source image should not deteriorate the average source image across all epochs.

For each sample s and event type c, the test is performed as follows: First, for each voxel n, a t-value is obtained using a one-sample t-test. This t-value $t_{s,c,n,0}$ scores the hypothesis that the mean voxel intensity across all E_c source images is zero (a zero-centered distribution of the positive voxel intensities can be created by normalization and log-transformation, both of which are described further below):

$$t_{s,c,n,0} = \frac{\overline{i_{s,c,*,n}}}{\sigma(i_{s,c,*,n})/\sqrt{E_c}}. \tag{5}$$

Then, for a total of R repetitions, the voxels within each source image are randomly shuffled. For each repetition r, this yields new randomized source images $I_{s,c,e,r}$, and new t-values $t_{s,c,n,r}$ can be computed according to

$$t_{s,c,n,r} = \frac{\overline{i_{s,c,*,r,n}}}{\sigma(i_{s,c,*,rn,})/\sqrt{E_c}}. \tag{6}$$

The standard deviation (SD) σ used for computing the t-values in equations 5 and 6 is special in that it is additionally spatially smoothed as described in Nichols and Holmes (2002). This smoothing may be performed by simply taking the average across all voxels, or alternatively using a smoothing kernel. After randomization, a significance threshold $t_{s,c}$ is computed as the $(1-p)\cdot 100^{\text{th}}$ percentile across repetitions, based on the largest t-values across all voxels per repetition. This maximum t-statistic controls the FWER and is a means of multiple comparison correction across voxels (Westfall & Young, 1993). For all voxels with $t_{s,c,n,0} < t_{s,c}$ the Null Hypothesis is confirmed, while for all other voxels consistency across epochs has been established. To visualize the locations-of-consistency, a t-statistic image can be generated based on $t_{s,c,n,0}$ where values of t below the significance threshold are set to zero.

The test for differences between event types is again performed independently for each sample. Here, the Null Hypothesis is that there is no difference between event types, i.e. that the same source images occur regardless of event type. If the Null Hypothesis holds, randomly perturbing source images across event types should not alter the average source images per event type.

For each sample s, the test is performed as follows: First, an F-test is performed using a one-way Analysis of Variance (ANOVA) for each voxel n where the event types c are regarded as factors (Maxwell & Delaney, 2004). The F-value $F_{s,n,0}$ thus obtained measures the hypothesis that the voxel means of all E_c source images per event type are equal. For R repetitions, source images are then randomly shuffled across event types. For each repetition r, randomized source images $I_{s,c,e,r}$ are obtained and F-values $F_{s,n,r}$ can be computed per voxel. Next, a significance threshold F_s is computed as the $(1-p)\cdot 100^{\text{th}}$ percentile across repetitions, based on the largest F-values across all voxels per repetition (maximum F-statistic). For all voxels with $F_{s,n,0} < F_s$ the Null Hypothesis is confirmed, while for all other voxels it has been established that they are significantly different. To visualize the locations of significance, an F-statistic image can be generated based on $F_{s,n,0}$ where values of F below the significance threshold are set to zero. Because a global measure of source image difference has been used, no further correction for multiple testing across voxels is necessary. While the F-test per se is known to be non-robust against deviations from normality, in the context of SnPM it is only the ordering of, not the absolute F values, that determine significance.

Again, a test for the significance of consecutive rejections of the Null Hypothesis can be performed (Koenig & Melie-García, 2009). Optionally, data may be collapsed across samples of interest to increase the SNR. Source images may be normalized and/or log-transformed before entering the calculations. Normalization allows comparing relative as opposed to absolute source magnitudes. A log-transformation can make the distribution of the (always positive) voxel intensities more symmetric and – if voxel intensities have previously been normalized so that their sum-of-squares equals the number of voxels – zero-centered. Neither normalization nor log-transformation are strictly required for CDR SnPM, though, as non-parametric statistics per se are robust with respect to unknown or skewed distributions (Nichols & Holmes, 2002). An extension to different categories of event types is possible using ANOVA for multiple factors (Maxwell & Delaney, 2004). CDR SnPM computation times scale linearly with number of samples, number of randomizations, and number of source locations.

CDR SnPM analysis was performed using the Curry software. Again, values of $p < 0.05$ were regarded as significant, with $R = 1000$ the number of repetitions. Source distribution normalization and log-transformation were used and σ-averaging was applied. Again, all of the differently filtered and decimated data sets were processed.

Multiple Comparison Correction

Neither TANOVA nor CDR SnPM per se require a multiple comparison correction across sensors or voxels, because complete voltage topography maps are used for TANOVA and a maximum statistic is employed in CDR SnPM. However, both methods are performed for each sample and neighboring samples yield to multiple compar-

isons, if the spectral content of the data is impaired by low-pass filtering or otherwise limited.

To assess the number of independent comparisons n that occur due to low-pass filtering the data but still analyzing each sample, one should keep in mind that, according to the Nyquist–Shannon sampling theorem, after filtering using a cutoff frequency of f_c, data may be resampled at $2f_c$ without losing information. If the original sampling frequency is f_s, there are $f_s/2f_c$ ways to perform this resampling depending on which out of $f_s/2f_c$ samples is picked as the first sample. This ratio equals the number of comparisons n to consider when analyzing low-pass filtered data sample by sample:

$$n = f_s/2f_c. \tag{7}$$

The corresponding multiple comparison-corrected significance level α using the Šidák correction is

$$\alpha = 1 - (1 - \bar{\alpha})^{1/n} = 1 - (1 - \bar{\alpha})^{2f_c/f_s} \tag{8}$$

with $\bar{\alpha}$ the experiment-wide significance level.

As a consequence, for the analysis of the low-pass filtered data sets with $f_c = 40\,\text{Hz}$ and $\bar{\alpha} = 0.05$, a corrected significance threshold of $\alpha = 0.0163$ was used, including an adapted number of repetitions $R = 50/\alpha = 3071$.

Simulated Data

In order to test the statistical methods, an additional simulated dataset was created, using the same electrode layout, sampling rate, prestimulus and post-stimulus times as described above for the CPT experiment. This dataset comprised 100 epochs each of two different types. One epoch type ("dipole + noise") was created by simulating a current dipole source in the postcentral gyrus, 15 mm beneath the inner skull layer of the same realistic BEM head model as described above (Fig 3). Its dipole moment was modeled to be zero before 0 ms and linearly rise to 100 µA mm at 500 ms. The second epoch type ("noise") contained zero data. White Gaussian noise with a standard deviation of 10 µV was added to all epochs. A second version of this simulated data set was obtained by applying a low-pass filter with $f_c = 10\,\text{Hz}$. For the statistical analyses described above, values of $p < 0.05$ were regarded as significant, the number of repetitions was $R = 1000$, and a corrected significance threshold of $\alpha = 0.0041$ according to Eq. 8 was used for $f_c = 10\,\text{Hz}$, with the corresponding adapted number of repetitions $R = 12210$.

In order to independently assess the TANOVA results for this simulated dataset, the time-varying SNRs for the first principal component (Hastie, Tibshirani, & Friedman, 2009) of the averaged "dipole + noise" epochs was plotted and latencies with an $\text{SNR} < 1$ were marked as insignificant. The first principal component was chosen because it represents the simulated dipole topography in this case where the simulated dipole is clearly large enough to dominate the noise. Before applying Principal Component Analysis (PCA), data were SNR-transformed (whitened) by multiplication with the inverse standard deviation of the noise, estimated from the signal-free latencies before 0 ms (R. Greenblatt, 1995; Fuchs et al., 1998).

Results

For the averaged "dipole + noise" epochs of the simulated dataset, the estimated standard deviation of the noise was $\sigma_{\text{noise}} = 1\,\mu\text{V}$. For the low-pass filtered version, $\sigma_{\text{noise}} = 0.231\,\mu\text{V}$.

For the low-pass filtered CPT data set, after excluding epochs with signals exceeding $\pm 30\,\mu\text{V}$,

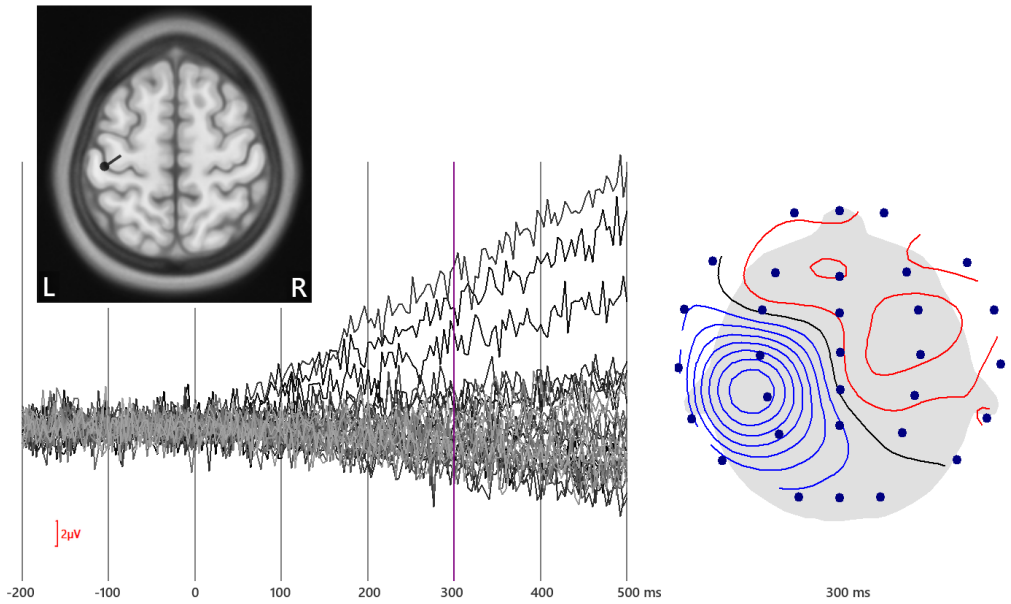

Figure 3: Simulated dipole location (top left), butterfly plot of the average "dipole + noise" waveforms (lower left) and voltage topography map for the 300 ms latency (right).

166 epochs remained: 34 of type "target" and 132 of type "distractor". Epoch counts for all other data sets derived from the CPT data are listed in the upper rows of Table 1. Data were subjected to TANOVA and sLORETA-based SnPM analyses.

Topographic Analysis of Variance

For the simulated dataset, the TANOVA consistency test (Fig. 4) established consistency of the "dipole+noise" epochs for all latencies after 84 ms, with additional, shorter periods of consistency from 60 to 64 ms and from 72 to 76 ms, as well as from -12 to -8 ms. Single significant samples failed the test for significance of contiguous rejections of the Null hypothesis, which in this case required a minimum of two samples. The "noise" epochs yielded no significant periods of consistency but a total of 9 isolated samples with $p < \alpha$. For comparison, the number of false positives to be expected is α times the number of samples which equals $0.05 \cdot 176 = 8.8$. The TANOVA test for differences between epoch types was satisfied from 92 ms onwards with the exception of the 129 ms sample. Again, two or more consecutively significant samples were required to establish significance of contiguous samples, and as a consequence 7 significant samples were rejected, including the 84 ms sample. The first principal component, when represented in SNR units, had an SNR ≥ 1 from 84 ms on.

In the case of the low-pass filtered CPT dataset, the TANOVA consistency test for the target stimuli yielded periods of consistency from -88 ms to -72 ms, from 60 ms to 68 ms and from 132 ms to 500 ms, with a total of 101 significant samples. For the distractors, consistency periods occurred from -140 ms to -112 ms, from -80 ms to -68 ms, from -56 ms to 120 ms, and from 132 ms to 500 ms. The total number of significant samples was 150. The test for differences between targets

Table 1: Dataset characteristics, significance levels, number of repetitions, and number of significant samples for TANOVA and CDR SnPM.

	Differently Filtered Datasets					Decimated No. Epochs		
Data Characteristics								
Low Cutoff [Hz]	0.15	0.15	1	2	3	0.15	0.15	0.15
High Cutoff [Hz]	125	40	40	40	40	40	40	40
Target No. Epochs	34	34	36	37	37	25	16	7
Distractor No. Epochs	131	132	154	158	158	100	67	35
Total No. Epochs	165	166	190	195	195	125	83	42
Statistics Parameters								
Significance Level α	0.05	0.0163	0.0163	0.0163	0.0163	0.0163	0.0163	0.0163
No. of Repetitions R	1000	3071	3071	3071	3071	3071	3071	3071
TANOVA	Samples $p < \alpha$							
Target	108	101	106	105	101	104	99	114
Distractor	156	150	137	122	116	132	115	87
Difference	67	57	64	66	65	64	55	35
CDR SnPM	Samples $p < \alpha$							
Target	147	139	162	168	161	117	73	45
Distractor	176	176	176	176	176	176	176	127
Difference	37	26	30	17	10	27	24	10

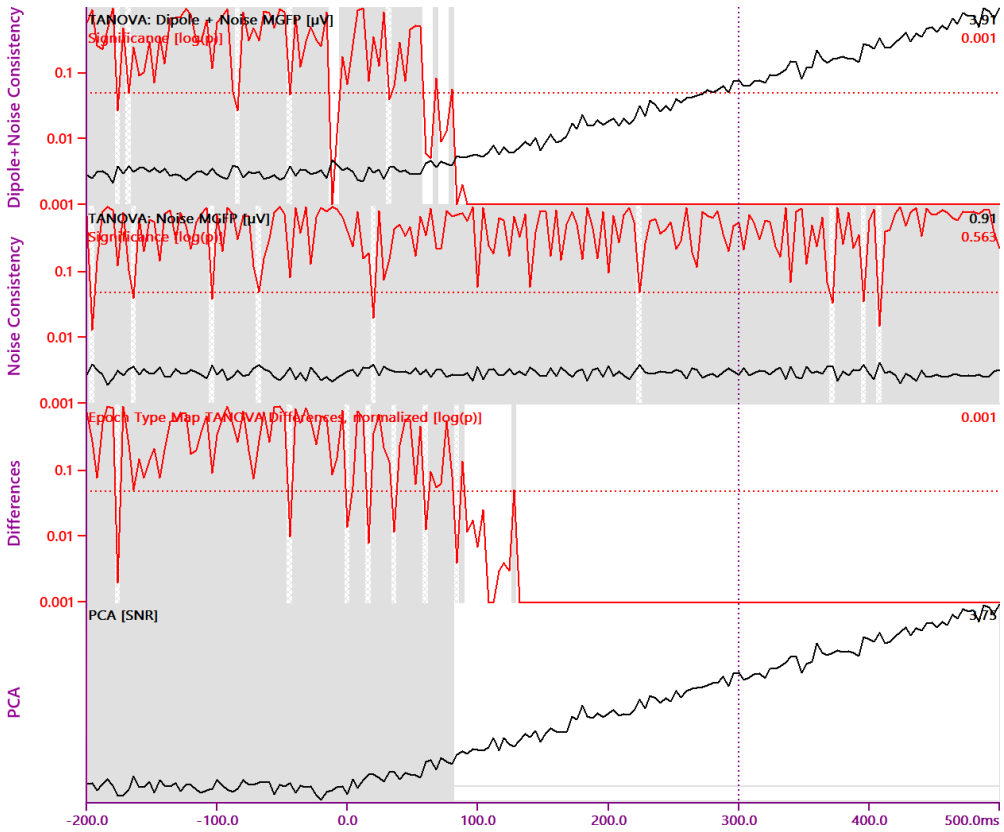

Figure 4: TANOVA results for the unfiltered simulated dataset. Red waveforms are p-Values depicted in a logarithmic scale, and white areas indicate significance, with $p < \alpha$. Short hatched gray areas indicate significance but failure to establish significance of consecutive rejections. The significance level $\alpha = 0.05$ is visualized as a horizontal red dotted line. Rows 1 and 2 show consistency test results for "dipole+noise" and "noise" epochs, respectively. Black waveforms are MGFPs of the average per event type, scaled equally. Row 3 shows differences between epoch types. Row 4 shows the SNR of the first principal component. Here, white areas mark SNRs ≥ 1. Numbers in the upper right corners of each waveform are the numerical values of that waveform for the 300 ms time point, indicated by a dotted vertical line.

and distractors yielded significance latencies from 164 ms to 184 ms, 204 ms to 380 ms, and 436 ms to 452 ms, and a total of 57 significant samples. A single significant sample at -76 ms was rejected because two or more contiguously significant samples were required to establish significance of consecutive rejections of the Null hypothesis. The results are shown in Fig. 5, and the number of significant samples is also presented in the TANOVA rows of Table 1. The computation time for the TANOVA tests with 3071 randomizations each for 31 EEG channels and 166 epochs, performed for all 176 samples per epoch at 250 Hz was 18 seconds on a 2.3 GHz Core i7-4850HQ CPU.

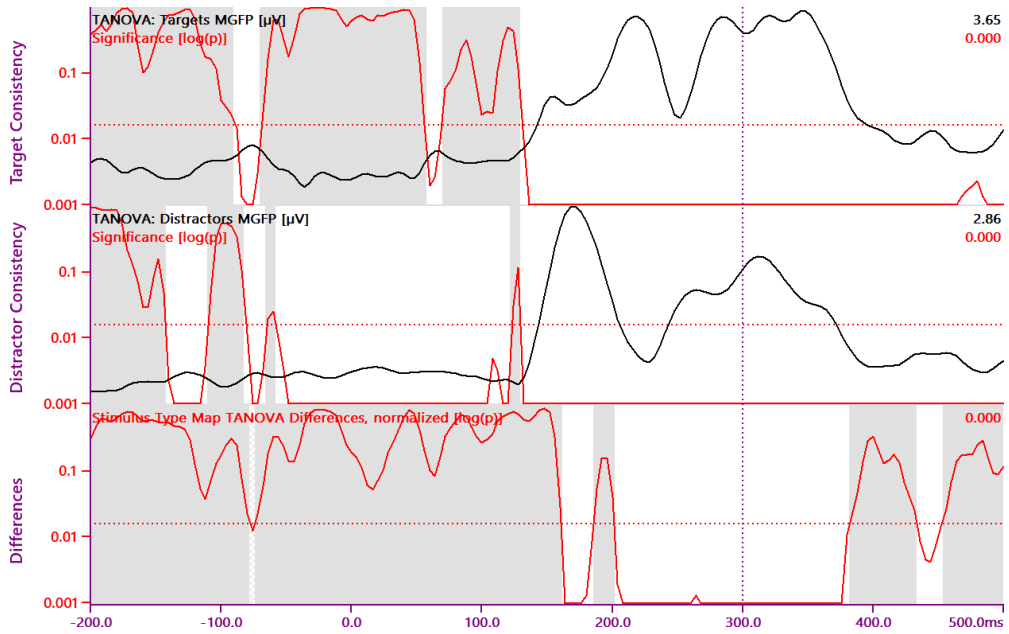

Figure 5: TANOVA results for the 40 Hz low-pass filtered CPT dataset. Red waveforms are p-Values depicted in a logarithmic scale, and white areas indicate significance, with $p < \alpha$. Short hatched gray areas indicate significance but failure to establish significance of consecutive rejections. The significance level $\alpha = 0.0163$ is visualized as a horizontal red dotted line. Rows 1 and 2 show consistency test results for target and distractor stimuli, respectively. Black waveforms are MGFPs of the average per stimulus type, scaled equally. Row 3 shows differences between targets and distractors. Numbers in the upper right corners of each waveform are the numerical values of that waveform for the 300 ms time point, indicated by a dotted vertical line.

Statistical non-Parametric Mapping

For the simulated dataset, consistency of the "dipole+noise" sLORETA results could be established for latencies from 180 ms on, with the exception of the 188 ms, 192 ms, and 204 ms samples. Single significant samples were rejected by the test for significance of contiguously significant samples, which required a minimum of two samples. The "noise" epoch consistency test failed, with a total of four single-sample false positives rejected. The test for differences of sLORETA results between epoch types yielded latencies of 196 ms and later, except for the 204 ms, 224 ms, and 228 ms samples. Results are shown in Fig. 6. The locations of significantly different activity between epoch types are illustrated in Fig. 7 for the 300 ms latency, with differences in the postcentral gyrus area and in the frontal lobes.

In the case of the low-pass filtered CPT dataset, the SnPM consistency tests established consistency (Null Hypothesis rejected for at least one voxel) for the target stimuli at a total of 139 out of 176 samples (-200 to -192 ms, -180 to -164 ms, -152 to -108 ms, -88 to -40 ms, -32 to 56 ms, 64 to 84 ms, 108 to 244 ms, 264 to 384 ms, 396 to 400 ms, 452 to 472 ms, 480 to 488 ms), and for the distractor stimuli at all samples. The test for

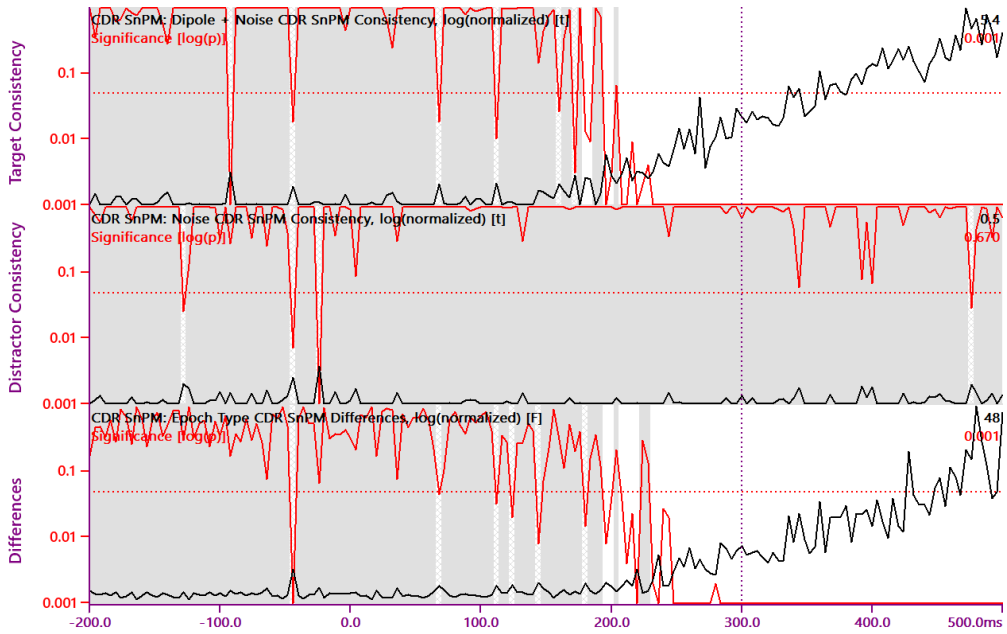

Figure 6: CDR SnPM results for the unfiltered simulated dataset. Red waveforms are p-Values depicted in a logarithmic scale, and white areas indicate significance, with $p < \alpha$. Short hatched gray areas indicate significance but failure to establish significance of consecutive rejections. The significance level $\alpha = 0.05$ is visualized as a horizontal red dotted line. Rows 1 and 2 show consistency test results for target and distractor stimuli, respectively. Black waveforms are the maximum t-values, scaled equally. Row 3 illustrates differences between targets and distractors. Here, the black waveform represents maximum F-values. The numbers in the upper right corners of each waveform are the numerical values of that waveform for the 300 ms time point, indicated by a dotted vertical line.

differences between targets and distractors yielded significant latencies (Null Hypothesis rejected for at least one voxel) from 172 ms to 180 ms, 228 ms to 244 ms, and 276 ms to 336 ms. Single significant samples at 148 ms and 344 ms were rejected because two or more contiguously significant samples were required to establish significance of consecutive rejections of the Null hypothesis. Results are presented in Fig. 8, and the number of significant samples is also presented in the SnPM rows of Table 1. Fig. 9 shows the spatial distribution of F-values above the significance level for the 300 ms time point, highlighting frontocentral and posterior right hemisphere differences. While the cerebellum was excluded from source analysis, some source symbols visually overlap with cerebellar areas due to the 7 mm resolution of the sLORETA source space. The computation of sLORETA CDR results for all epochs and samples took 40 seconds. Computation times for the CDR SnPM tests for all epochs and samples and 3071 randomizations were 33 minutes, of which 7 minutes and 10 seconds were used for the CDR SnPM difference analysis.

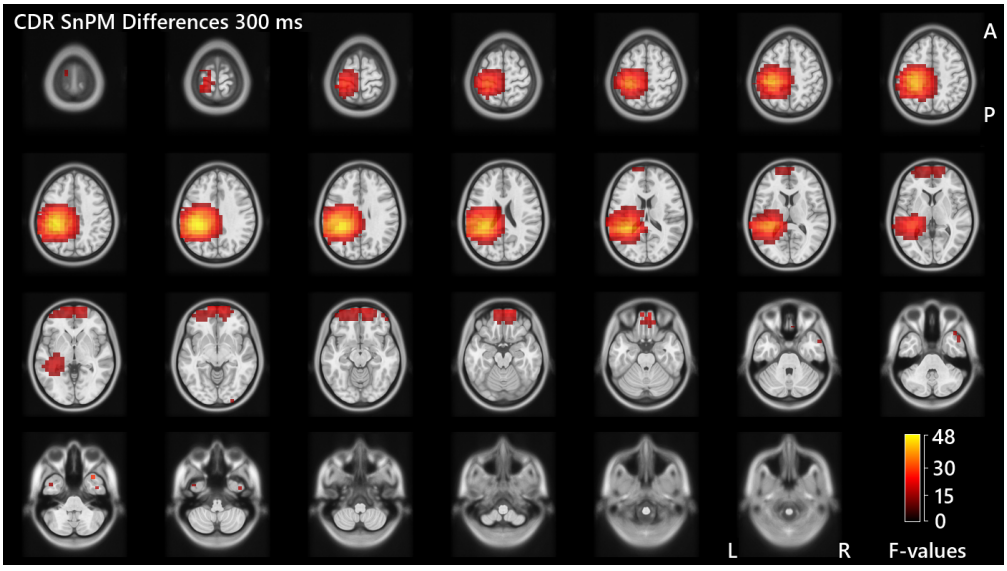

Figure 7: CDR SnPM F-values for the unfiltered simulated dataset. Thumbnails show template MRI slices ordered from top to bottom, with labels indicating axis orientations where A represents anterior, P posterior, L left, and R right. Red-yellow colored overlays are the significance-thresholded F-value image for the 300 ms latency.

Different Filter Frequencies and Epoch Counts

For the simulated dataset, Fig. 10 shows a comparison of the TANOVA and CDR SnPM difference tests already summarized above with results for a version of the dataset low-pass filtered at 10 Hz. While for the unfiltered dataset, significant TANOVA differences start at 92 ms, the filtered dataset yields significant differences already from 28 ms onwards. Both latencies are in line with the PCA results, where the SNR of the first principal component representing the simulated dipole map rises above one at 84 ms and 28 ms, respectively. The CDR SnPM differences show less sensitivity with significance established at 196 ms and 88 ms, respectively.

The results of submitting differently filtered versions of the CPT dataset to TANOVA and CDR SnPM difference tests are shown in Fig. 12. The second row of these figures represents the same 40 Hz low-pass filtered dataset that was characterized above and presented in Figs. 5 and 8. Table 1 summarizes the number of significant samples for both tests. For high-pass filter frequencies of 2 Hz and 3 Hz, the number of significant samples is reduced for the CDR SnPM tests (Fig. 11a). The impact of filtering on the TANOVA results is smaller compared to CDR SnPM. For the less-filtered data, more prestimulus samples are significant. Significant differences for the 300 ms latency cannot be detected for the 3 to 40 Hz-filtered dataset.

Reducing the number of epochs yields the results shown in Fig. 13 (here the top row represents the same dataset as in Figs. 5 and 8), as well as in Table 1. For only 42 epochs, the overall number of significant samples is markedly reduced (Fig. 11b), while for TANOVA, with smaller epoch

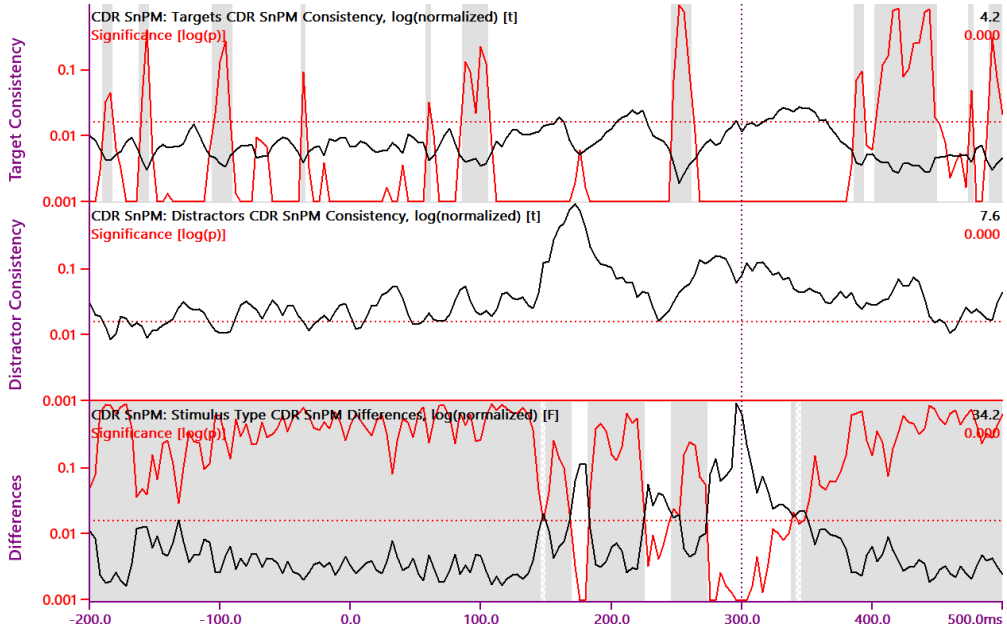

Figure 8: CDR SnPM results for the 40 Hz low-pass filtered CPT dataset. Red waveforms are p-Values depicted in a logarithmic scale, and white areas indicate significance, with $p < \alpha$. Short hatched gray areas indicate significance but failure to establish significance of consecutive rejections. The significance level $\alpha = 0.0163$ is visualized as a horizontal red dotted line. Rows 1 and 2 show consistency test results for target and distractor stimuli, respectively. Black waveforms are the maximum t-values, scaled equally. Row 3 illustrates differences between targets and distractors. Here, the black waveform represents maximum F-values. The numbers in the upper right corners of each waveform are the numerical values of that waveform for the 300 ms time point, indicated by a dotted vertical line.

counts, more pre-stimulus samples were found significant. A significant difference for the 300 ms latency cannot be established.

Discussion

For the simulated dataset, TANOVA identified latencies of consistency within epoch type for the "dipole+noise" epochs, while for the "noise"-only epochs just the expected number of false positives was reported, none of which passed the test for contiguous rejections of the Null hypothesis. Latencies with significant differences between epoch types agreed with latencies where the SNR of the first principal component of the averaged "dipole+noise" epochs exceeded 1.

CDR SnPM, when applied to the simulated dataset, highlighted two distinct brain regions of significant differences, one of them in the post-central gyrus area showing hyper-activity, the other in the frontal lobe area with hypo-activity, due to the sharper fall-off beyond the maxima of sLORETA activity for the "dipole+noise" epochs as compared to the "noise"-only epochs where the smoothing-effect of regularization dominates the sLORETA images due to lack of features in the data.

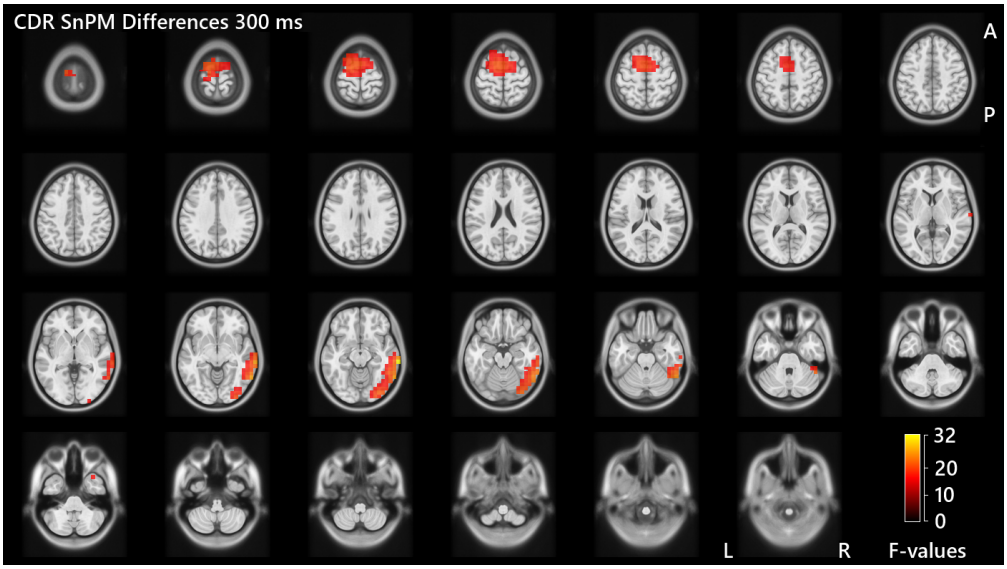

Figure 9: CDR SnPM F-values for the 40 Hz low-pass filtered CPT dataset. Thumbnails show template MRI slices ordered from top to bottom, with labels indicating axis orientations where A represents anterior, P posterior, L left, and R right. Red-yellow colored overlays are the significance-thresholded F-value image for the 300 ms latency.

The sensitivity of CDR SnPM was lower compared to TANOVA, which can be seen from the later onset of the respective periods of significant latencies in the difference tests. The maximum statistic used in CDR SnPM summarizes the individual voxel statistics into a single measure, thus addressing the spatial multiple comparison problem while at the same time retaining spatial resolution. Nichols and Holmes (2002) describe a tradeoff between statistical power and the ability to localize significant voxels. Thus, the lower sensitivity of SnPM as compared to TANOVA, which employs an omnibus measure to summarize map topography, may be explained. Furthermore, scalp topography maps contain information about source orientation, while the voxel intensities analyzed in CDR SnPM do not. It is beyond the scope of this paper to clarify whether the differences in statistical outcome between TANOVA and CDR SnPM observed here are due to the transition to source space, the representation of source activity as absolute values, or the maximum statistic employed to elicit locations of significance. It should be noted, however, that the outcome of sLORETA source localization are not oriented sources but voxel intensities. Rather, sLORETA was chosen because of its low localization error, its uniform spatial sensitivity due to the inherent normalization to the standard deviation per voxel, and because its outcome has been shown to be robust with respect to changes in the regularization parameter. The spatial resolution to be expected from CDR SnPM depends on the underlying source analysis method, with "low resolution" even a part of the sLORETA acronym. When just a representation of significant peaks as source images is required – as opposed to establishing significance for certain source locations – a

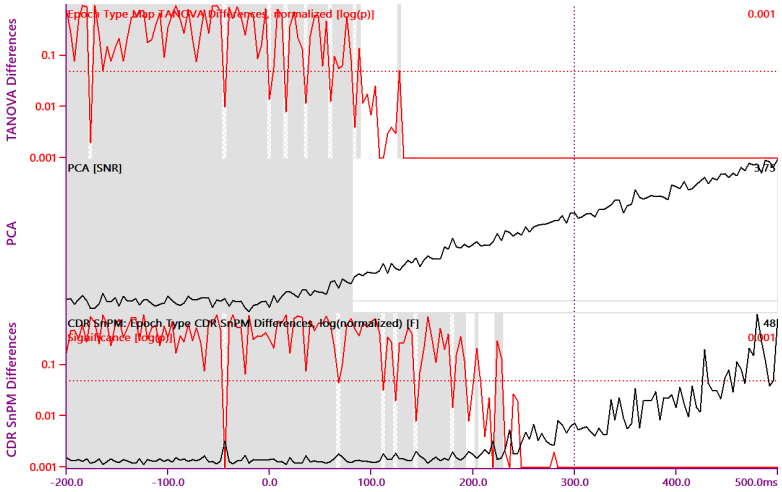

(a) Unfiltered dataset.

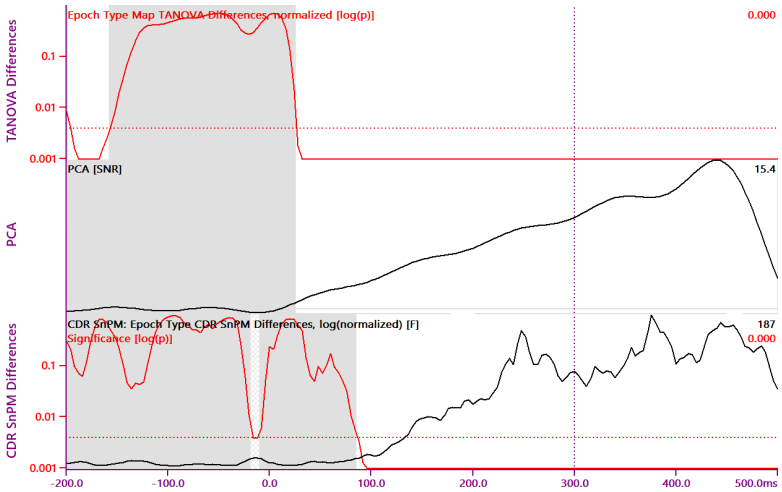

(b) 10 Hz low-pass filtered dataset.

Figure 10: Comparison of difference test results for the unfiltered and 10 Hz low-pass filtered simulated datasets. Red waveforms are p-Values depicted in a logarithmic scale, and white areas indicate significance, with $p < \alpha$. Short hatched gray areas indicate significance but failure to establish significance of consecutive rejections. The significance levels α are visualized as horizontal red dotted lines. Row 1 shows TANOVA results. Row 2 shows the SNR of the first principal component, where white areas mark SNRs ≥ 1. Row 3 are CDR SnPM results, where the black waveform represents maximum F-values.

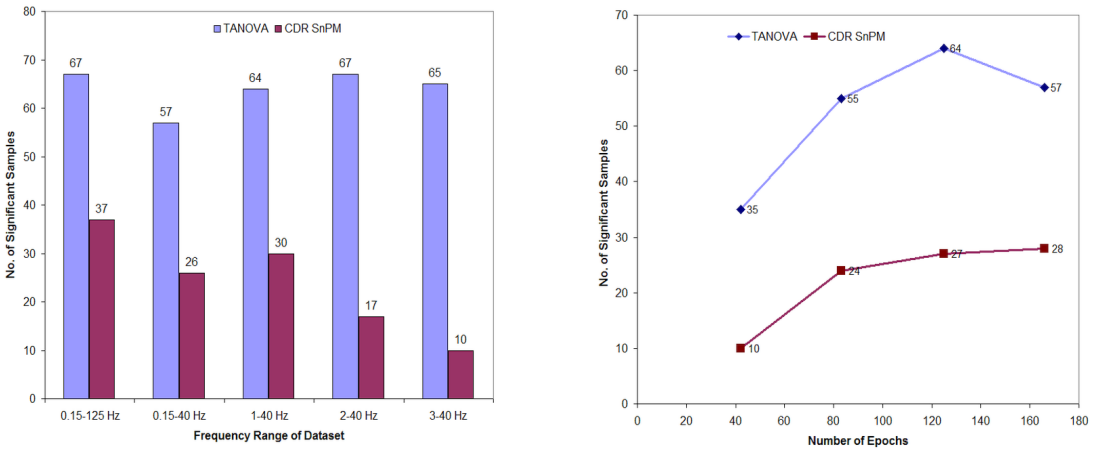

(a) Differently filtered datasets.

(b) Different epoch counts.

Figure 11: Number of significant samples for the TANOVA and CDR SnPM difference tests for a) differently filtered datasets and b) different epoch counts.

dipole or current density analysis of the samples-of-significance identified by TANOVA would be an alternative strategy to CDR SnPM.

The visual CPT data showed sufficient consistency within stimulus type to warrant a comparison of the different stimulus types. The TANOVA method, which processes complete voltage topography maps, detected significant differences between stimulus types for more latencies than the CDR SnPM method. TANOVA uses an omnibus measure of map topographies for establishing significance, with the consistency test Null hypothesis that random maps have been measured. There are certainly situations, where, even without stimulus-related brain activity, map topographies are not completely random. Examples would be subjects with strong alpha in a group of posterior electrodes or residual muscle spiking in temporal electrodes, which may both show up as significant consistencies. The TANOVA consistency test should therefore not be seen as an indication of proper artifact reduction or removal. In the case of the CPT data, when looking at the TANOVA consistency test results and also at the difference tests for small epoch counts, significant pre-stimulus latencies can be observed. Without ISI randomization, it is common for slow effects to show up as consistent signals in the pre-stimulus latencies. Even with ISI randomization, as used in this study, such effects may not be totally suppressed, especially for the Bereitschaftspotential (Gladwin, Lindsen, & Jong, 2006). Furthermore, an amplifier-side 0.15 Hz high-pass filter was used in this study, while a comparison of the differently filtered datasets showed how, with increasing high-pass filter frequencies, the number of pre-stimulus significances became smaller, indicating the additional possibility of dispersion caused by low-frequency high-pass filtering, of which the commonly used baseline correction is just a special case.

CDR SnPM was able to extract brain locations with significantly different sLORETA activations between target and distractor stimuli. The time

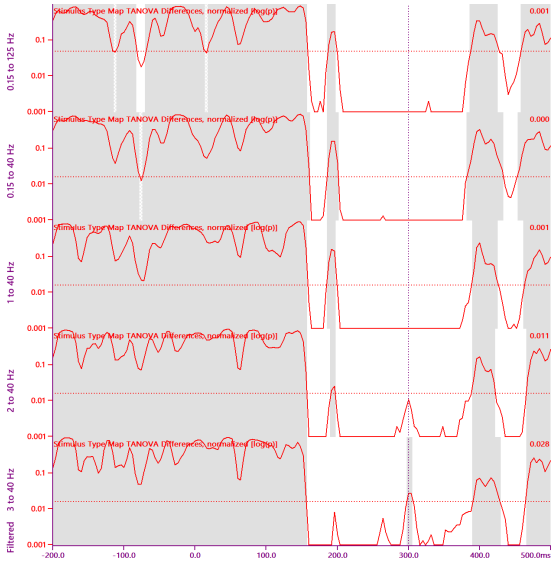

(a) TANOVA.

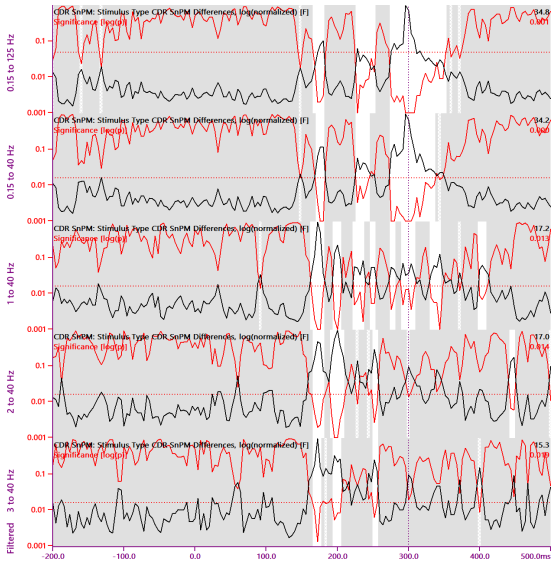

(b) CDR SnPM: black waveforms represent maximum F-values.

Figure 12: Comparison of difference test results for the differently filtered CPT datasets. Red waveforms are p-Values depicted in a logarithmic scale, and white areas indicate significance, with $p < \alpha$. Short hatched gray areas indicate significance but failure to establish significance of consecutive rejections. The significance levels α are visualized as horizontal red dotted lines. a) TANOVA b) CDR SnPM: black waveforms represent maximum F-values.

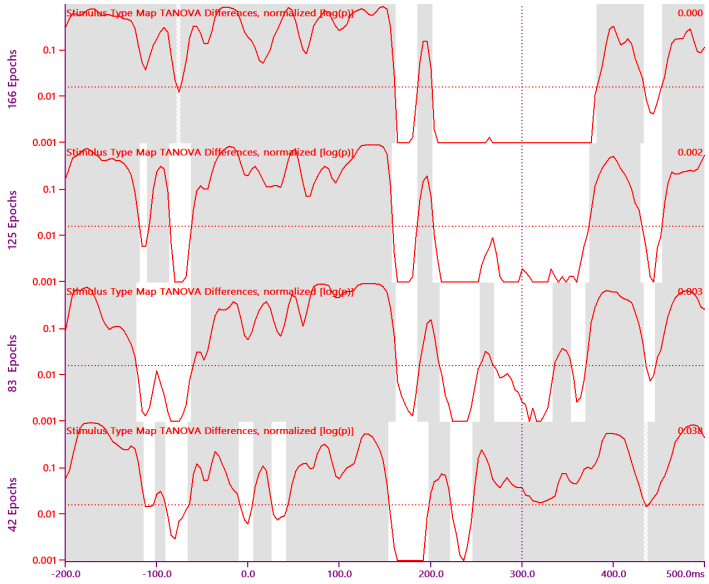

(a) TANOVA .

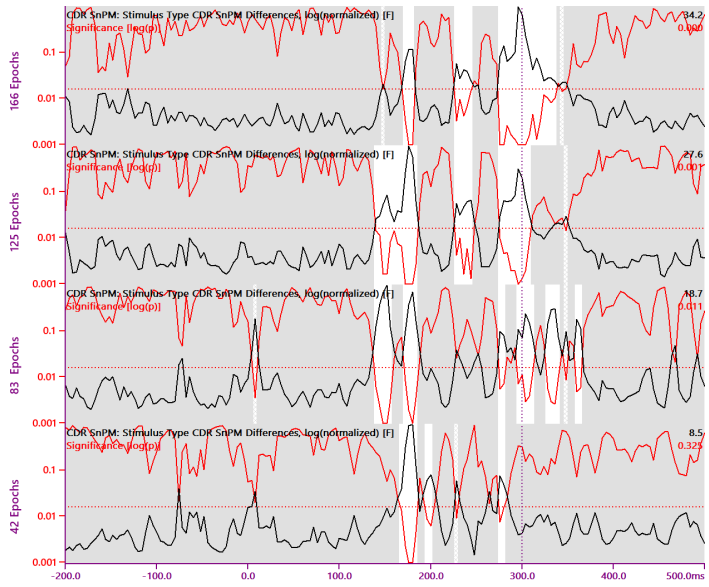

(b) CDR SnPM: black waveforms represent maximum F-values

Figure 13: Comparison of difference test results for different epoch counts of the 40 Hz low-pass filtered CPT dataset, with consecutive rows showing results for all, 75 %, 50 %, and 25 % of epochs used for the analysis. Red waveforms are p-Values depicted in a logarithmic scale, and white areas indicate significance, with $p < \alpha$. Short hatched gray areas indicate significance but failure to establish significance of consecutive rejections. The significance level $\alpha = 0.0163$ is visualized as horizontal red dotted lines. a) TANOVA b) CDR SnPM: black waveforms represent maximum F-values.

ranges and brain regions uncovered for the 300 ms latency are consistent with what is known about the P300, with frontocentral and posterior right hemisphere differences (Bledowski et al., 2004). The results of CDR SnPM consistency tests are of limited value beyond establishing that the underlying source images are suited for difference testing, as they show consistency for nearly all samples. This can be an effect of regularization, which for noisy data produces smooth source images of small amplitude, which are then amplified by normalization.

Filtering EEG data is a well-established technique for changing waveform morphology in such a way as to accent characteristic peaks for visual inspection, or to enhance SNR by low-pass filtering the data. With the low-pass filtered simulated dataset and temporal multiple comparison correction, the effects of this SNR enhancement are clearly visible. Significance could be established for earlier latencies with smaller dipole activity as for the unfiltered simulated data. This is corroborated by the very similar latencies where the SNR of the first principal component exceeded 1. In general, however, filtering disseminates signal energy onto nearby samples and can potentially impair features in the data that may be crucial for establishing significance. While TANOVA results were less affected by filtering, CDR SnPM seems to work best on slightly or unfiltered data. For the CPT dataset analyzed in this study, epoch counts of 125 and higher produced more significant samples than epoch counts of 83 and lower. One possible extrapolation of this observation is, that the number of epochs generally accepted as sufficient for creating average ERPs is also sufficient for performing TANOVA and SnPM analyses.

The proposed method for multiple comparison correction in the time domain uses the ratio between twice the maximum frequency in the data and the sampling rate as its comparison count parameter. A corrected significance threshold is used if this ratio is smaller than one, leading to higher numbers of required repetitions and longer computation times. The question of how to choose or estimate the maximum frequency remains to be discussed. If data have previously been filtered, as is the case in most ERP/ERF studies, an upper limit for the maximum frequency is certainly given by the low-pass filter frequency and transition width. As the observed brain processes might work on even slower scales, it becomes clear that this is by no means a conservative method for multiple comparison correction. However, it accounts at least for the common practice of recording data at 1 or 2 kHz but later low-pass filtering to some 40 or 70 Hz, which effectively reduces environmental noise. Consequently, in this paper only the low-pass filter frequency was used for determining the significance threshold.

Conclusion

It was shown how TANOVA and CDR SnPM can be applied to the individual epochs obtained in an ERP experiment. The TANOVA analysis established data plausibility and identified latencies-of-interest for further analysis. The SnPM analysis, in addition, identified brain regions of consistent activity within stimulus type and of significantly different activity between stimulus types.

Obviously, the approach presented here is not limited to EEG data analysis but can also be performed on MEG data. It can easily be extended to group or longitudinal studies. In some cases, it is then necessary to shuffle within-subject only. For group or longitudinal studies, either individual averages per stimulus type can be processed,

or all acquired epochs of all datasets. Furthermore, SnPM can be employed to identify significant channels when performed on voltage topographies instead of source distributions.

References

Bledowski, C., Prvulovic, D., Hoechstetter, K., Scherg, M., Wibral, M., Goebel, R., et al. (2004). Localizing p300 generators in visual target and distractor processing: a combined event-related potential and functional magnetic resonance imaging study. *J Neurosci*, *24*(42), 9353–9360.

Fuchs, M., Wagner, M., & Kastner, J. (2001). Boundary element method volume conductor models for eeg source reconstruction. *Clin Neurophysiol*, *112*(8), 1400–1407.

Fuchs, M., Wagner, M., Köhler, T., & Wischmann, H. A. (1999). Linear and nonlinear current density reconstructions. *J Clin Neurophysiol*, *16*(3), 267–295.

Fuchs, M., Wagner, M., Wischmann, H. A., Köhler, T., Theissen, A., Drenckhahn, R., et al. (1998). Improving source reconstructions by combining bioelectric and biomagnetic data. *Electroencephalogr Clin Neurophysiol*, *107*(2), 93–111.

Gladwin, T. E., Lindsen, J. P., & Jong, R. de. (2006). Pre-stimulus eeg effects related to response speed, task switching and upcoming response hand. *Biol Psychol*, *72*(1), 15–34.

Greenblatt, R. (1995). Biomagnetism: fundamental research and clinical applications. In C. Baumgartner, L. Deecke, G. Stroink, & S. Williamson (Eds.), (pp. 402–405). Amsterdam: Elsevier Science / IOS Press.

Greenblatt, R. E., & Pflieger, M. E. (2004). Randomization-based hypothesis testing from event-related data. *Brain Topogr*, *16*(4), 225–232.

Hastie, T., Tibshirani, R., & Friedman, J. (2009). *The elements of statistical learning: Data mining, inference, and prediction* (2nd ed.). NY: Springer.

Kim, J. S., Han, J. M., Park, K. S., & Chung, C. K. (2008). Distribution-based minimum-norm estimation with multiple trials. *Comput Biol Med*, *38*(11-12), 1203–1210.

Kim, Y. Y., Roh, A. Y., Namgoong, Y., Jo, H. J., Lee, J.-M., & Kwon, J. S. (2009). Cortical network dynamics during source memory retrieval: current density imaging with individual mri. *Hum Brain Mapp*, *30*(1), 78–91.

Koenig, T., & Melie-García, L. (2009). Electrical neuroimaging. In C. Michel, T. Koenig, D. Brandeis, L. Gianotti, & J. Wackermann (Eds.), (pp. 169–189). Cambridge: Cambridge University Press.

Koenig, T., & Melie-García, L. (2010). A method to determine the presence of averaged event-related fields using randomization tests. *Brain Topogr*, *23*(3), 233–242.

Maxwell, S. E., & Delaney, H. D. (2004). *Designing experiments and analyzing data: A model comparison perspective* (2nd ed.). Mahwah, NJ: Lawrence Erlbaum Associates.

Murray, M. M., Brunet, D., & Michel, C. M. (2008). Topographic erp analyses: a step-by-step tutorial review. *Brain Topogr*, *20*(4), 249–264.

Murray, M. M., Michel, C. M., Peralta, R. G. de, Ortigue, S., Brunet, D., Andino, S. G., et al. (2004). Rapid discrimination of

visual and multisensory memories revealed by electrical neuroimaging. *Neuroimage*, *21*(1), 125–135.

Nichols, T. E., & Holmes, A. P. (2002). Nonparametric permutation tests for functional neuroimaging: a primer with examples. *Hum Brain Mapp*, *15*(1), 1–25.

Pantazis, D., Nichols, T. E., Baillet, S., & Leahy, R. M. (2003). Spatiotemporal localization of significant activation in meg using permutation tests. *Inf Process Med Imaging*, *18*, 512–523.

Pascual-Marqui, R. D. (2002). Standardized low-resolution brain electromagnetic tomography (sloreta): technical details. *Methods Find Exp Clin Pharmacol*, *24 Suppl D*, 5–12.

Wagner, M. (2014). Magnetoencephalography. In S. Supek & C. J. Aine (Eds.), (chap. Non-Parametric Statistical Analysis of Map Topographies on the Epoch Level). Heidelberg: Springer. (In Press)

Wagner, M., Fuchs, M., & Kastner, J. (2004). Evaluation of sloreta in the presence of noise and multiple sources. *Brain Topogr*, *16*(4), 277–280.

Wagner, M., Fuchs, M., Wischmann, H., Ottenberg, K., & Dössel, O. (1995). Biomagnetism: fundamental research and clinical applications. In C. Baumgartner, L. Deecke, G. Stroink, & S. Williamson (Eds.), *Biomagnetism: Fundamental research and clinical applications: Proceedings of the 9th international conference on biomagnetism* (pp. 352–356). Amsterdam: Elsevier Science / IOS Press.

Westfall, P., & Young, S. (1993). *Resampling-based multiple testing: Examples and methods for p-value adjustment* (Vol. 279). John Wiley & Sons.

Abstracts of the 22nd German EEG/EP Mapping Meeting, Giessen, October 11 – 13, 2013

States and Kalman Filters T. Sauer *Lehrstuhl für Mathematik mit Schwerpunkt Digitale Bildverarbeitung, Universität Passau*

Kalman-Filter sind ein hochinteressantes Verfahren zur Analyse von Zeitreihen, die auf der Basis eines stochastischen Modells Daten zu erklären versuchen, indem sie den wahrscheinlichsten Zustand bestimmen. Hat man ein gutes Modell der zu untersuchenden Daten zur Verfügung, lassen sich so Rauschen und Ausreißer sehr gut unterdrücken.

Wavelet-Design S. Flüggen (1), A. Klein (1), T. Sauer (2), W. Skrandies (1) *(1) Justus-Liebig-Universität Gießen, Deutschland (2) Universität Passau, Deutschland*

Bei der Analyse von EEG-Daten ist es von Interesse die Veränderung der auftretenden Frequenzbänder zu analysieren. Häufig wird dafür die schnelle Fourier Transformation genutzt. Dabei ist jedoch nicht ersichtlich zu welcher Zeit die Frequenzen im untersuchten Signal auftreten. Dies ist mit Hilfe der Wavelettransformation möglich. Mit ihr lassen sich Aussagen über die zeitliche Verschiebung der auftretenden Frequenzbänder in einem EP treffen.

Bei der Wavelettransformation werden Korrelationen zwischen verschobenen und gestreckten bzw. gestauchten Versionen des gewählten Wavelets und dem Signal berechnet. Je größer die Ähnlichkeit des Signals und des Wavelets ist, umso größer ist der Wert der Wavelettransformation. Da die im Wavelet auftretenden Frequenzen bekannt sind, ist es somit möglich Aussagen über die Frequenzen im zu untersuchenden Signal zu treffen.

Die Wavelettransformation lässt in der Wahl des Wavelets viele Freiheiten. Die bekannten Wavelets wie das Morlet Wavelet oder das Maxican Hat Wavelet werden in vielen Anwendungen genutzt, sind aber nicht überall optimal. Bei der Suche nach bestimmten Effekten in Signalen ist es günstiger ein Wavelet genau an die gesuchte Form anzupassen. Diese Anpassung lässt sich beispielsweise mit Hilfe so genannter "gieriger Algorithmen" umsetzen, genauer mit Hilfe der m-Term-Approximation. Dabei ist die Implementierung der Wavelettransformation mit Hilfe der FFT und weiteren Hilfsmitteln effizient und stabil möglich.

Detecting eye-movement artefacts with extreme value statistics A. Klein, W. Skrandies *Physiologisches Institut, Justus-Liebig-Universität Gießen*

Das Erkennen von Augenbewegungsartefakten ist eine der häufigsten Aufgaben in der Vorverarbeitung von EEG-Daten. Zur Identifikation von Blinzelartefakten kommt dabei häufig ein Schwellenwertkriterium zum Einsatz, das Artefakte als das Überschreiten einer bestimmten Amplitude, beispielsweise 50 µV an einem der frontalen Kanäle, definiert. Ein solches Verfahren auf Basis einer absoluten Amplitude als Schwelle verbraucht natürlich fast keine Rechenzeit, ist jedoch insofern ungünstig, als es keinerlei Rücksicht auf interindividuelle Schwankungen der Artefakt- und EEG-Amplituden nimmt. Andererseits sind einfache statistische Tests dadurch erschwert, dass einerseits die statistische Verteilung des EEGs nur schwer analytisch abzubilden ist, und andererseits meist auch keine passende

Null-Stichprobe zur Verfügung steht, aus der entsprechende Parameter abgeleitet werden könnten. Eine Lösung dieser Probleme bietet die Extremwertstatistik, die es aufgrund der dort auftretenden Verteilungen ermöglicht, epochenweise parametrische Tests ohne aufwendige Parameterschätzungen durchzuführen. Wir stellen ein entsprechendes Verfahren vor und vergleichen anhand der Daten von 55 Versuchspersonen seine Effektivität mit dem oben genannten 50 µV-Kriterium. Zusammenfassend kann gesagt werden, dass die vorgeschlagene Methode Augenbewegungsartefakte zuverlässig erkennen kann und so als automatisches und objektives Verfahren für die Artefakterkennung eingesetzt werden kann.

Hilbert-Transformation: Zeitvariante Analyse von Amplituden-Frequenzkopplungen und Phasenkopplungen H. Witte *Universitätsklinikum der Friedrich-Schiller Universität Jena*

Die Hilbert-Transformation (HT) wird für die lineare zeitvariante Analyse von Einkomponenten-Signalen mit sehr enger Bandpasscharakteristik verwendet. Sie ist deshalb für die Analyse von transienten, oszillatorischen Hirnaktivitäten geeignet, die als amplituden- und frequenz(phasen)modulierte Schwingungen beschrieben werden können. In der Regel ist eine zusätzliche Bandpassfilterung unumgänglich, um diese Bedingungen einhalten zu können. Ergebnis der Analyse mittels HT ist die Hüllkurve (=Momentanamplitude, Amplitudendemodulation) und die Momentanphase bzw. -frequenz (Phasen- bzw. Frequenzdemodulation). Die Momentanfrequenz ist die erste zeitliche Ableitung der Momentanphase. Die Verläufe der Hüllkurve und der Momentanfrequenz können für so genannte „cross-frequency"-Analysen (Amplituden-Amplituden-, Amplituden-Frequenz- sowie Frequenz-Frequenz-Kopplungen) zwischen Frequenz-komponenten eines Signals bzw. zwischen Signalen verwendet werden. Die Momentanphase dient als Grundlage für Phasenkopplungs- bzw. Phasensynchronisationsanalysen. Die Momentanverläufe können aus dem komplexen analytischen Signal errechnet werden, wofür die HT eingesetzt wird. Als Realteil des analytischen Signals wird das gemessene und gefilterte Signal verwendet und der Imaginärteil wird über die HT erzeugt. Es wird gezeigt, wie der Imaginärteil im Zeitbereich und im Frequenzbereich berechnet werden kann. Beispiele aus dem Bereich der Analyse transienter EEG-Muster und der Spikeanalyse zeigen die typischen Anwendungsbereiche der HT. Die Nachteile der HT sind, dass man den Frequenzbereich für die Analyse kennen muss und dieser dann fest eingestellt bleibt. Vorteil ist, dass der Frequenzbereich auf die Oszillation individuell zugeschnitten werden kann. Signaladaptive Ansätze, wie zum Beispiel die Hilbert-Huang-Transformation (HHT), kompensieren diesen Nachteil. Aus der Anwendung der HHT resultieren jedoch andere Nachteile. Der Zusammenhang zwischen der Gabor,- der Morlet-Wavelet-Transformation, der HT, der HHT und anderen zeitvarianten Verfahren wird in Wacker und Witte (2013) gezeigt.

Wacker, M., Witte, H.: Time-frequency techniques in biomedical signal analysis: A tutorial review of similarities and differences. Meth Inf Med 52(2013) doi:10.3414/ME12-01-0083.

Zeitvariante multivariate autoregressive Modellierung: Analyse der funktionellen und effektiven Hirnaktivität L. Leistritz, H. Witte *Universitätsklinikum der Friedrich-Schiller Universität Jena*

Die multivariate autoregressive (MVAR) Modellierung des EEG ist seit langem für die Konnek-

tivitätsanalyse aus EEG-Registrierungen etabliert, wobei die aus den AR-Modellparametern errechneten Konnektivitätsmaße ungerichtete (z.B. Kohärenz) und gerichtete Interaktionen (z. B. Granger Causality (GC), partial directed coherence (PDC)) Interaktionen zwischen den Signalen aufdecken können. Weiterhin kann zwischen nicht frequenzselektiven (z.B. GC) und frequenzselektiven Maßen (z. B. PDC) unterschieden werden. Nachdem die MVAR-Modellierung in das breite Spektrum der Methodenansätze zur Konnektivitätsanalyse eingeordnet worden ist, werden deren Voraussetzungen und Grundlagen charakterisiert sowie die Konzepte für die GC und PDC für das bivariate AR-Modell dargestellt. Mit Hilfe von Methoden für die adaptive Schätzung der Modellparameter gelingt es, zeitvariante GC- und PDC-Analysen durchzuführen. Damit kann die Zeitdynamik der Hirn-Konnektivität kognitiver Prozesse untersucht werden. Die Signal-Zustandsraum-Darstellung ist die Grundlage für den Kalman-Filter-Ansatz, der sehr hohe Dimensionen (Kanäle) für die zeitvariante MVAR-Modellierung ermöglicht. Es werden Studien auf der Grundlage von Analysen im Sensor (Elektroden)- und im Quellenraum (Quellenaktivitäten) vorgestellt. Weiterhin wird gezeigt, dass die zeitvarianten Methoden auch für single-shot-fMRT-Daten anwendbar sind. Die Dimensionsreduktion der Ergebnisse der Konnektivitätsanalyse (signifikante Interaktionen) kann durch graphentheoretische Methoden erreicht werden. Die Grenzen und die Nachteile des zeitvarianten MVAR-Ansatzes werden umfassend diskutiert. Hierfür liegt eine aktuelle Studie von Leistritz et al. (2013) für die PDC vor.

Leistritz, L., Pester, B., Doering, A., Schiecke, K., Babiloni, F., Astolfi, L., Witte, H.: Time-variant Partial Directed Coherence for analyzing connectivity: a methodological study. Phil.Trans. R. Soc. A 317(2013)

Molecular genetic associations with Positive Emotionality A.J.L. Munk (1), C. Wielpütz (1), E.M. Müller (2), J. Hennig (1) *(1) Abteilung für Differentielle Psychologie und Persönlichkeitsforschung; Abteilung für Klinische Psychologie (2) Fachbereich für Psychologie und Sportwisschenschaften, Justus-Liebig-Universität Gießen*

As previous ERP studies with an emotional Stroop paradigm concentrated mainly on detecting differences between several ERP components and interindividual differences in the reaction to threatening or negative words in comparison to neutral ones, we wanted to test, if these differences also occurred in response to positive in comparison to neutral words. On a neurophysiological level, dopamine is known to be associated with certain aspects of Positive Emotionality. Therefore we postulate that there are different systems within the construct of Positive Emotionality in dependence of the meaning of different positive emotions. As the DRD2 dopamine receptor gene has been associated with differences in reward sensitivity and incentive motivation, we hypothesized that reaction to positive words would vary according to variants of the DRD2 and category of the positive word, indicating a very early stage of different processing of emotional valent stimuli. Emotions such as "lust" and "anticipation" should be associated to dopamine, whereas emotions regarding attachment and warmth could be more related for example to the oxytocinergic system.

To test our hypotheses, we recorded an electroencephalogram ($N = 69$) while subjects completed an emotional stroop task. The stroop task included positive and neutral words. Positive words were categorized in "lust", "anticipation", and "closeness". To assess different reac-

tions to positive and neutral words, we calculated peaks and amplitudes for the LPP. A higher amplitude in the LPP for positive words was revealed. Moreover, we detected significant interactions between DRD2 genotype and the emotional word categories "lust" ($p < .05$) and "anticipation" ($p < .05$), but not for "closeness" in comparison neutral words in the LPP. These results point to interindividual differences in the processing of positive emotional stimuli on a very basal, neurophysiological level.

rTMS in the treatment of panic disorder - neurobiological and clinical effects S. Deppermann (1), N. Vennewald (2), F.B. Häußinger (1), S. Sickinger (1), A.C. Ehlis (1), A.J. Fallgatter (1), P. Zwanzger (2) *(1) Klinik für Psychiatrie und Psychotherapie, Tübingen (2) Klinik für Psychiatrie und Psychotherapie, Münster*

As many anxiety disorders panic disorder is characterized by hyperactivity of the amygdala as well as well as hypoactivity of the prefrontal cortex. Even though cognitive behavioral therapy (CBT) has been shown to be an effective option in many cases additional care as for example the treatment with selective serotonin re-uptake inhibitors is necessary. However, the onset of treatment effects are delayed and not all patients are compliant with medical therapy. This is why we investigated repetitive transcranial magnetic stimulation (rTMS) as another possible add-on to CBT. To do so we recruited 20 healthy controls and 40 patients with panic disorder who received CBT in terms of group therapy. Half of them were also treated with an activating rTMS protocol over the left dorsolateral prefrontal cortex during the first three weeks of therapy whereas the other half received placebo treatment. Before and after rTMS all subjects underwent near-infrared spectroscopy (NIRS) measurement while performing emotional as well as cognitive tasks. NIRS is an optical imaging method which depicts changes in brain activation patterns in terms of blood oxygenation levels and can hence show whether active rTMS resulted in higher normalization of prefrontal hypoactivation compared to the placebo group. The final results of the study will be presented during this conference.

Hemodynamics and Electrophysiology of Error Processing in Healthy Heavy Social Drinkers under the influence of visual alcoholic stimuli A.M. Kroczek, F.B. Häußinger, T. Dresler, L.H. Ernst, AJ. Fallgatter, A.-C. Ehlis *Klinik für Psychiatrie und Psychotherapie, Tübingen*

Eine Dysregulation der Verhaltensüberwachung kann sich in verschiedenen Psychopathologien äußern, wodurch zentralnervöse Korrelate der Fehlerverarbeitung insbesondere für die Psychiatrie von großer Relevanz sind. So stehen z.B. Abhängigkeitserkrankungen mit einem unteraktivierten Verhaltensüberwachungssystems in Zusammenhang.

Die im Anterioren Cingulären Cortex (ACC) generierte error negativity (Ne)/error-related negativity (ERN) ist ein ereigniskorreliertes Potential (EKP), das mit Fehlerverarbeitung assoziiert wird. Des Weiteren sind auch Strukturen wie der dorsolaterale präfrontale Kortex (dlPFC) grundlegend an der Fehlerverarbeitung beteiligt. Die Aktivität in beiden Regionen lag im Fokus der Analysen. Für die aktuelle Studie wurden simultane NIRS-EEG Messungen durchgeführt, um die Stärken beider Methoden für die Untersuchung der Fehlerverarbeitung zu nutzen. Die zeitlich sehr hoch aufgelösten elektrophysiologischen Korrelate der Fehlerverarbeitung konnten so in Zusammenhang gebracht werden mit der hämodynamischen Aktivität in kortikalen Arealen.

Die Studie wurde an einer Population gesunder sozialer Viel- und Wenigtrinker durchgeführt.

Es zeigte sich ein positiver Zusammenhang zwischen der ERN-Amplitude in Fehler-Trials und einem Anstieg der dlPFC-Aktivierung in Trials, die auf einen Fehler folgten. Auf Verhaltensebene zeigten sich gleichzeitig verlängerte Reaktionszeiten nach einem Fehler (post-error slowing), die – in Übereinstimmung mit einer erhöhten Aktivierung des dlPFC – ebenfalls als Zeichen gesteigerter kognitiver Kontrolle nach fehlerhaften Reaktionen interpretiert werden können. NIRS scheint dabei geeignet zu sein, diese Kontrollprozesse – zusätzlich zu den über EEG-Maße erhobenen Monitoring-Prozessen im ACC – abzubilden.

Ein weiteres Konzept, das innerhalb der Studie untersucht werden sollte, ist die Cue-Reaktivität nach Alkoholreizen. In Studien mit alkoholabhängigen Patienten konnte gezeigt werden, dass alkoholische Reize sowohl zentralnervös, wie auch peripherphysiologisch, automatische Reaktionen hervorrufen können. Ein Einfluss alkoholischer Reize konnte auch in der aktuellen Stichprobe gesunder Vieltrinker gefunden werden, anhand verringerter ERN-Amplituden bei Fehlern nach Betrachtung alkoholischer Reize.

Neben interessanten Einflüssen auf die Hämodynamik weisen die Ergebnisse darauf hin, dass sich das Trinkverhalten auf elektrophysiologische Korrelate der Fehlerverarbeitung auswirkt, die sich noch nicht auf der Verhaltensebene äußern.

Laser-evoked potentials as a tool to measure descending inhibition (DNIC) with differential modulation of the underlying generators U. Baumgärtner, C. von der Heydt, R.-D. Treede *Chair of Neurophysiology, Centre for Biomedicine and Medical Technology Mannheim, Medical Faculty Mannheim, Heidelberg University, Mannheim, Germany*

Diffuse noxious inhibitory control (DNIC) describes the inhibition of pain by heterotopic noxious stimulation as has been shown in electrophysiological studies in animals and man. In this study, we aimed to analyze the effect of the cold-pressor test (CPT) on pain perception and evoked brain potentials and their underlying generators induced by nociceptive specific laser stimuli.

Twenty-four healthy volunteers were investigated in 2 sessions on separate days. Each session comprised 7 blocks of 30 brief nociceptive laser stimuli (energy 480-540 mJ; interstimulus interval 8-12 s) applied to the right hand dorsum with a break of 5 min between blocks. After the second block, the left hand was immersed either in ice water (3 °C; cold-pressor condition) for 2 minutes or in warm water (34 °C; control condition). These two sessions were balanced across subjects. Pain intensity ratings were acquired following each laser stimulus. In 16 out of these 24 volunteers we recorded laser-evoked potentials (LEP) during the 7 blocks in both sessions using a 32 channel EEG (bandpass 0.3-70 Hz, SR 1 kHz). The EEG was segmented into epochs ranging from -500 ms (pre-stimulus) till 1500 ms (post stimulus) and averaged blockwise separately for both conditions (CPT and control).

Amplitudes and latencies of surface potentials (T7-Cz and Cz-linked ears) were determined as well as location, amplitudes and latencies of activities of the 4 dipole generators obtained after source analysis (BESA 5.1).

Apart from a significant generalised habituation effect on LEP amplitudes and source activities across all blocks, the CPT caused an additional decrease in pain ratings, LEP amplitudes and source activities of 13 % on average compared

with the control condition during the first and/or second block following CPT. The effects lasted approximately 15 minutes. With respect to localization of the generators assigned to the bilateral operculo-insular cortex (OIC), mid-cingulate and contralateral parietal cortex, dipole shifts after CPT occurred in the OIC clearly in posterior direction and in mid-cingulate cortex slightly in superior direction.

These data show that LEP and pain ratings show both habituation and short-lasting suppression during/after tonic pain, and hence may serve as tool to quantify DNIC effects. For the first time, a differential effect of the underlying brain generators could be demonstrated with different time courses and changes in localisation following CPT. Supported by DFG Tr 236/13-4

Kortikale Oxygenierungsmuster gesunder Alterungsprozesse L.D. Müller, M.J. Herrmann *Klinik für Psychiatrie, Psychosomatik und Psychotherapie der Universität Würzburg, Würzburg*

Verglichen mit jungen Erwachsenen zeigen Probanden mit zunehmendem Alter abweichende Aktivierungsmuster im frontalen und parietalen Kortex. Die zugrundeliegenden Alterungsprozesse werden im Rahmen von Kompensations- und Dedifferenzierungsmechanismen sowie unspezifischer Aktivierung verschiedener Gehirnregionen diskutiert.

Zur genaueren Untersuchung dieser Prozesse, wurden zwei neuropsychologische Tests für Messungen mit der funktionellen Nahinfrarotspektroskopie (fNIRS) implementiert und die Gehirnaktivierung gesunder junger (18 – 32 Jahre) und älterer Probanden (64 – 77 Jahre) miteinander verglichen. Eine modifizierte Form des Trailmaking Tests (TMT) diente zur Messung des frontalen Kortex und ein Winkeldiskriminationstest (WDT) zur Erhebung der parietalen Kortexaktivierung.

Während des TMTs zeigen sich in beiden Gruppen Aktivierungen in dorso- und ventrolateralen präfrontalen Strukturen (vlPFC und dlPFC). Bei älteren Probanden zeigt sich jedoch eine geringere rechts hemisphärische Lateralisierung der dlPFC Aktivierung im Vergleich zu jüngeren Probanden. Bezüglich des WDT zeigen beide Gruppen inferior parietale Kortexaktivierung. Mit zunehmender Aufgabenschwierigkeit werden zusätzlich präfrontale Strukturen aktiviert. Diese zusätzliche frontale Aktivierung ist bei älteren Probanden stärker ausgeprägt als bei jüngeren Probanden während die parietale Aktivierung in älteren Probanden geringer ist.

Während die Ergebnisse des TMT mit dem bestehenden Hemispheric Asymmetry Reduction in Older Adults (HAROLD) Model (Cabeza, 2002) überein stimmen, entsprechen die Ergebnisse des WDT dem Posterior-Anterior Shift in Aging (PASA) Model (Davis et al, 2008).

Die hier beschriebenen Resultate tragen mit zwei bisher noch nicht im alt-jung Vergleich untersuchten Paradigmen zum Verständnis von gesunden Alterungsprozessen bei und können als Basis für die Untersuchung pathologischen Alterns herangeführt werden.

Near-infrared spectroscopy (NIRS) in psychiatry – Current developments A.-C. Ehlis, S. Schneider, F.B. Häußinger, T. Dresler, A.J. Fallgatter *Psychophysiology & Optical Imaging, Psychiatric University Hospital Tübingen, Tübingen*

Over the past two decades, near-infrared spectroscopy (NIRS) has been increasingly used to conduct functional activation studies in healthy subjects as well as patients with different neuropsychiatric disorders, most prominently schizophrenic illnesses, affective disorders and developmental syndromes, such as attention-

deficit/hyperactivity disorder as well as normal and pathological aging. This talk will give a brief overview of state of the art NIRS research in psychiatry covering different applications, including studies on the phenomenological characterization of psychiatric disorders, descriptions of life-time developmental aspects, treatment effects, and genetic influences on neuroimaging data. Moreover, new developments and promising future applications of NIRS in psychiatry will be discussed along with methodological shortcomings and corresponding analytical strategies. We conclude that NIRS is a valid addition to the range of neuroscientific methods available to assess neural mechanisms underlying neuropsychiatric disorders, with specific methodological advantages in certain investigational contexts. Future research should focus on expanding the presently used activation paradigms and cortical regions of interest, while additionally fostering technical and methodological advances particularly concerning the identification and removal of extracranial influences on NIRS data. Eventually, NIRS might be a useful tool in practical psychiatric settings involving both diagnostics and the complementary treatment of psychological disorders using, for example, neurofeedback applications.

Using Near-Infrared Spectroscopy (NIRS) for Brain-Computer Interface (BCI) Systems G. Bauernfeind, S.C. Wriessnegger, G.R. Müller-Putz *Institut für Semantische Datenanalyse/Knowledge Discovery*, *Technische Universität Graz*, *Österreich*

Near-infrared spectroscopy (NIRS) is an emerging non-invasive optical technique for the in-vivo assessment of cerebral oxygenation. In recent years multichannel NIRS has been used to study functional activity of the human cerebral cortex to cognitive, visual and motor tasks and appears to be becoming an established diagnostic tool in neonatology, pediatrics, psychiatry and neurorehabilitation. In addition to studying brain functions, NIRS has been increasingly used for brain computer interface (BCI) systems in the past years.

A BCI provides the user with artificial output channels to control external devices by the regulation of brain activity. Coyle et al. were the first to investigate the suitability of NIRS systems for next-generation BCIs, the so called optical BCI (oBCI) systems. Since that time, a few research groups have investigated different concepts using NIRS alternatively to, or in combination with (for the first time implemented by the Graz BCI Lab), traditional EEG-based systems for BCI communication and control. However, there is still ongoing research needed to investigate the full potential of NIRS in this field. For example, several studies showed the feasibility of using motor imagery for oBCI systems, but also other mental tasks, such as mental arithmetic or music imagery, exhibit potential as suitable control tasks. Therefore, it is of interest investigating brain activity during the performance of such mental tasks, addressing the questions which areas are involved, and how the activity changes over time. Furthermore, a common challenge for BCIs is a stable and reliable classification of single-trial data, especially for mental tasks. Therefore it is essential to improve the signal to noise ratio (SNR) and to reduce false classifications which may occur in the case of NIRS primarily due to misclassification of physiological noise.

Hybrid NIRS-EEG Brain Computer Interfaces J. Mehnert, S. Fazli, B. Blankertz *Informatik, TU Berlin*

Non-invasive Brain Computer Interfaces (BCI) have been promoted to be used for neuropros-

thetics. However, reports on applications with electroencephalography (EEG) show a demand for a better accuracy and stability. Here we investigate whether near-infrared spectroscopy (NIRS) can be used to enhance the EEG approach. In our study both methods were applied simultaneously in a real-time Sensory Motor Rhythm (SMR)-based BCI paradigm, involving executed movements as well as motor imagery. We tested how the classification of NIRS data can complement ongoing real-time EEG classification. Our results show that simultaneous measurements of NIRS and EEG can significantly improve the classification accuracy of motor imagery in over 90 % of considered subjects and increases performance by 5 % on average ($p<0.01$). However, the long temporal delay of the hemodynamic response may hinder an overall increase of bitrates. Furthermore we find that EEG and NIRS complement each other in terms of information content and are thus a viable multimodal imaging technique, suitable for BCI.

A Wearable Multi-Channel fNIRS System for Brain Imaging in Freely Moving Subjects S.K. Piper (1,2), A. Krueger (1), S.P. Koch (1), J. Mehnert (1,2), C. Habermehl (1,2), J. Steinbrink (1,2), H. Obrig (3,4), C.H. Schmitz (1,5) *(1) Charité University Medicine Berlin, Department of Neurology, Berlin, Germany (2) Charité University Medicine Berlin, Center for Stroke Research Berlin, Germany (3) Max Planck Institute for Human Cognitive and Brain Sciences, Leipzig, Germany (4) Clinic for Cognitive Neurology, University Hospital Leipzig, Germany (5) NIRx Medizintechnik GmbH, Berlin, Germany*

Functional near infrared spectroscopy (fNIRS) is a versatile neuroimaging tool with an increasing acceptance in the neuroimaging community. While often lauded for its portability, most of the fNIRS setups employed in neuroscientific research still impose usage in a laboratory environment. We present a wearable, multi-channel fNIRS imaging system for functional brain imaging in unrestrained settings. The system operates without optical fiber bundles, using eight dual wavelength light emitting diodes and eight electro-optical sensors, which can be placed freely on the subject's head for direct illumination and detection. Its performance is tested on $N = 8$ subjects in a motor execution paradigm performed under three different exercising conditions: (i) during outdoor bicycle riding, (ii) while pedaling on a stationary training bicycle, and (iii) sitting still on the training bicycle. Following left hand gripping, we observe a significant decrease in the deoxyhemoglobin concentration over the contralateral motor cortex in all three conditions. A significant task-related DHbO2 increase was seen for the non-pedaling condition. Although the gross movements involved in pedaling and steering a bike induced more motion artifacts than carrying out the same task while sitting still, we found no significant differences in the shape or amplitude of the HbR time courses for outdoor or indoor cycling and sitting still. We demonstrate the general feasibility of using wearable multi-channel NIRS during strenuous exercise in natural, unrestrained settings and discuss the origins and effects of data artifacts. We provide quantitative guidelines for taking condition-dependent signal quality into account to allow the comparison of data across various levels of physical exercise. To the best of our knowledge, this is the first demonstration of functional NIRS brain imaging during an outdoor activity in a real life situation in humans. (http://dx.doi.org/10.1016/j.neuroimage.2013.06.062)

Correction for extra-cranial fNIRS signals F.B. Häußinger, T. Dresler, A.-C. Ehlis, A. Fallgat-

ter *Uniklinik für Psychiatrie und Psychotherapie Tübingen, Deutschland*

Functional near-infrared spectroscopy (fNIRS) is an optical neuroimaging method that detects temporal concentration changes of oxygenated (oxy) and deoxygenated (deoxy) hemoglobin within the cortex, so that neural activation can be deduced. But fNIRS has to be shown to be confounded by systemic compounds with extra-cranial origin, like changes in blood pressure. Especially event-related signal pattern induced by vaso-constriction of fronto-polar veins impairs the inference of frontal brain activation elicited by cognitive tasks using fNIRS. We conducted a simultaneous fNIRS-fMRI study with a working memory paradigm (n-back) to examine this problem and to develop a filter method for such extra-cranial impairments. For it, we identified channel of the forehead probe arrangement mainly mapping extra-cranial hemodynamics to correct for skin blood flow. Additionally the data was corrected for motion artifacts. Applying these filters, the ability of fNIRS was substantially improved to infer functional brain activation in frontal brain areas. These results imply that in future fNIRS studies measuring functional brain activation in the forehead region need to consider different filter approaches to correct for extra-cranial signals.

Crossmodale Verarbeitung visueller und auditorischer Reize gemessen mit NIRS

M.M. Plichta (1), A.B.M. Gerdes (2), M.J. Wieser (3), A.J. Fallgatter (4), G.W.A. Alpers, (2) *(1) Zentralinstitut für Seelische Gesundheit, Medizinische Fakultät Mannheim/Universität Heidelberg, Mannheim (2) Lehrstuhl für Klinische und Biologische Psychologie, Universität Mannheim (3) Lehrstuhl für Biologische Psychologie, Klinische Psychologie und Psychotherapie, Universität Würzburg (4) Universitätsklinik für Psychiatrie und Psychotherapie, Universität Tübingen*

Während Studien zur multimodalen Wahrnehmung von auditorischen und visuellen Informationen in der experimentellen Psychologie eine lange Tradition haben, gibt es bisher nur wenige Studien, die emotionales Material unterschiedlicher Modalitäten verwenden. Hinweise auf wechselseitige Einflüsse unterschiedlicher sensorischer Modalitäten legen nahe, dass auch die Darbietung emotionaler Reize in einer sensorischen Modalität, Verarbeitungsprozesse anderer Modalitäten verändern könnte.

Die vorliegende Studie soll untersuchen, ob und wie die gleichzeitige Darbietung von emotionalen Bildern und Geräuschen die Aktivität in visuellen und auditorischen Kortexarealen wechselseitig beeinflusst.

Einer Gruppe von 15 Versuchspersonen wurden positive, neutrale und negative Bilder (IAPS) in Kombination mit jeweils einem positiven, negativen, oder neutralen Geräusch (IADS) präsentiert. Während der Präsentation wurde die Aktivität im auditorischen und visuellen Kortex mittels funktioneller Nah-Infrarot-Spektroskopie (fNIRS) gemessen. Im Anschluss wurden alle präsentierten Stimuluskombinationen hinsichtlich Valenz und Arousal bewertet.

Die vorläufigen Analysen zeigen, dass emotionale Geräusche unabhängig vom zeitgleich präsentierten Bild stärker im auditorischen Kortex verarbeitet werden als neutrale Geräusche, während emotionale Bilder stärker im visuellen Kortex verarbeitet werden. Die Analyse der Bewertungen von Valenz und Arousal der Geräusch-Bild-Kombinationen zeigen, dass der emotionale Gehalt der Bilder stärker die Gesamtbewertung beeinflusst als der emotionale Gehalt der

Geräusche. Die Überprüfung, ob sich dies auch in der neuronalen Aktivität zeigt steht noch aus. Mögliche Implikationen für Emotionsverarbeitungsprozesse werden diskutiert.

Quantitative Electric Brain Maps (Enkephaloglyphs) connected to Eye-Tracking Results W. Dimpfel, H-C. Hofmann *NeuroCode AG, Wetzlar, Deutschland*

Goal of the investigation was to connect eye-tracking to online EEG analysis within a project dedicated to validate this approach for market research. Twenty subjects were asked to view a presentation containing a memory test, a Stroop-test and an image comparison as cognitive challenges. In addition, several video film clips as well as TV commercials were included as an emotional challenge. The presentation lasted about 19 minutes. During this time quantitative EEG (neo-CATEEM®, MEWICON CATEEM-Tec) was recorded continuously together with eye-tracking (NYAN Software, Interactive Minds). After Fast Fourier Transformation values were calculated in percent of the median of corresponding values from every location giving an enkephaloglyph. A comparison between the classic analyses using a sweep length of 4000 ms with 364 ms of the fast mode was performed using data from a signal generator. Using the classic approach very sharp transitions from one to the next frequency band were documented. Using the new approach identical maps and power density distributions were seen in the middle of a frequency band. However, transitions between specially defined frequency ranges turned out to be somewhat slower. This validation is documented as a video. Single enkephaloglyphs of 364 ms duration contained immense focal increases of spectral power in various brain regions. Performance of memory tasks was associated with large increases of left frontal delta power interpreted as mental activation. Performance of the Stroop-test led to enhanced beta2 power at temporal electrode position T3 and T4, which is interpreted as enhanced tension. Comparison of two images led to high spectral theta power within the occipital lobe related to higher visual perception and awareness. Discriminant analysis of female versus male data from all electrode positions uncovered totally separate clusters for both genders. Thus, fast real time online dynamic EEG analysis providing about 3 images/second produces reliable results.

The topography of potentials visually evoked by learned Japanese symbols under the influence of odors B. Würzer, A. Klein, W. Skrandies *Physiologisches Institut, Justus-Liebig-Universität Gießen, Deutschland*

This study intended to show electrophysiological effects of odors on visually evoked potentials and their topography within a learning task. In addition, it was designed to test the ability of odors to serve as contextual information in the sense of environmental context-dependent memory or environmental reinstatement. The experiment included two phases. Phase 1 included a recording session prior to learning and the vocabulary learning itself. Phase 2 covered the period in which both the second recording session and the memory test took place. The odor conditions were „no odor“ (plain air – plain air), „congruent“ (lemon – lemon) and „incongruent“ (lemon – spruce). The German meaning of those 40 black and white symbols had to be learned within 20 minutes in between the two recording sessions. A lab specific array with 30 electrodes was used for the 41 participants. The interstimulus interval was zero milliseconds, the stimulus presentation time 1000 milliseconds. There was no significant effect of „odor condition“ on behavioral performance and

hence no context-dependent memory effect. By the use of Global Field Power, five components of event related electrical brain activity with mean latencies of 117, 215, 407, 704 and 865 ms after stimulus onset were defined. The analysis was focused on the latency, GFP-amplitude and the location of Centroids. A P100-like component with distinct differences to checkerboard VEP-P100 is described. The ANOVA revealed effects of time, learning and odour condition and complex interactions. Especially the latency of the early components at 117 and 215 ms was shorter when the environmental scent was changed from lemon to spruce ("incongruent") suggesting expedited information processing. Learning effects could clearly be seen in an early (117 ms) and a late component (704 ms) the latter showing a hemispheric effect. Furthermore, a kind of habituation caused topographic alterations in the two earlier components as a result of time or repetitive stimulation. To sum up, this study clearly shows how components of VEPs are altered by odour and learning effects and their interactions.

Multitasking and error processing
X. Weißbecker-Klaus *BAuA (Bundesanstalt für Arbeitsschutz und Arbeitsmedizin), Berlin*

Ausgehend von der nicht weg zu denkenden Präsenz von Multitaskinganforderungen an modernen Computerarbeitsplätzen, wurde experimentell eine Doppelaufgabensituation mit einer visuell-manuellen und einer auditiv-verbalen Anforderung konstruiert. Die Computertätigkeit häufig unterbrechenden verbalen Zusatzinformationen (über Telefonate oder persönliche Ansprachen) sind oftmals Quellen fehlerhafter Arbeitsschritte, die die Qualität und Sicherheit der Arbeit unter Umständen entscheidend beeinträchtigen können. Im Fokus der Untersuchung stehen Fehlerverarbeitungsprozesse, deren ungestörter Ablauf, auch bei gleichzeitiger Verarbeitung semantischer Inhalte, gewährleistet werden muss, um folgenschwere Fehlschritte zu entdecken und korrigieren zu können.

Um die womögliche Beeinträchtigung der Fehlerverarbeitungsprozesse in Multitaskingsituationen zu untersuchen und eventuelle altersabhängige Differenzen zu erfassen, wurden zwei Probandengruppen erwerbsfähigen Alters (20- bis 35-Jährige und 50- bis 65-Jährige) während der gleichzeitigen Bearbeitung einer modifizierten Flankeraufgabe und einer lexikalen Entscheidungsaufgabe untersucht. Neben Verhaltensdaten (Reaktionszeiten, Fehleranzahl und Post-error slowing) wurden ausgewählte Komponenten Ereigniskorrelierter Potentiale erhoben (ERN, Pe, N400).

Es konnte gezeigt werden, dass die Flankeraufgabe bei simultaner Zusatzanforderung mit kürzeren Reaktionszeiten, jedoch einer höheren Fehlerquote gelöst wurde. Die fehlerhaften Flankertrials gingen nicht nur mit verzögerten Antwortlatenzen in der lexikalen Entscheidungsaufgabe einher, sondern verursachten eine Verschiebung der N400 Peak-Amplitude um mehr als 400 ms. Die Prozesse der Fehlerverarbeitung und der semantischen Integration konnten somit nicht gleichzeitig im ZNS verarbeitet werden. Des Weiteren beeinflusste die semantische Anforderung die Fehlerverarbeitung in der Parallelaufgabe:

Während sich das Post-error slowing in der Einfachaufgabenbedingung deutlich abzeichnete, zeigte sich bei der simultanen semantischen Informationsverarbeitung keine adaptive Verhaltenskontrolle mehr nach Fehlern. Darüber hinaus ließ die Reduktion der Pe Peak-Amplituden unter Multitasking auf eine Beeinträchtigung der bewussten Fehlererkennung schließen.

Insgesamt zeigen sich deutliche Interferenzen bei paralleler Aufgabenbearbeitung, die nicht nur die Ausführung der Einzelaufgaben beeinträchtigen, sondern auch die Fehler-verarbeitungsprozesse. Bei bewusstseinspflichtigen Prozessen ist zur Vermeidung potentiell schwerwiegender Fehlschritte, von Multitasking abzuraten.

Topographie "Feedback-bezogener" elektrischer Hirnaktivität W. Skrandies, A. Klein *Physiologisches Institut, Justus-Liebig-Universität Gießen*

Wir untersuchten die "Feedback-bezogenen" evozierten Potentiale in einem Experiment, in dem 19 junge Erwachsene mathematische Aufgaben lösen mussten. Das EEG wurde in 30 Kanälen registriert, während "Teilbarkeits-Aufgaben" auf einem Monitor präsentiert wurden. In einer Pause wurde den Teilnehmern der Lösungsweg erklärt, so dass die Messungen in eine Phase vor und nach dem Lernen aufgeteilt werden konnten. Die Versuchspersonen gaben ihre Antworten per Knopfdruck, und die Rückmeldung über eine richtige oder falsche Antwort erfolgte über einen hohen oder tiefen Ton. Der Zeitpunkt der Rückmeldung diente als Trigger für die gemittelten "Feedback-bezogenen" evozierten Potentiale.

Eine negative Komponente mit einer mittleren Latenz von etwa 110 ms tauchte frontal in der Mittellinie auf. Weder Stärke noch Topographie dieser Komponente unterschieden sich in den verschiedenen Bedingungen. Wir untersuchten die Unterschiede der elektrischen Hirnaktivität, die durch Rückmeldung richtiger oder falscher Antworten hervorgerufen wurde. Dabei fanden wir verschiedene Komponenten zwischen 210 und 470 ms, die signifikante Unterschiede in der Topographie aufwiesen. Alle Unterschiede waren nach dem Lernen deutlicher als zu Beginn des Experiments.

Zwischen 210 und 250 ms gab es hauptsächlich über frontalen Bereichen eine FRN-ähnliche Komponente. Die Aktivität zwischen 210 und ms, 270 und 350 ms, 370 und 390 ms, sowie zwischen 410 und 470 ms zeigte signifikante Unterschiede. Diese Effekte fanden sich jedoch eher über zentralen, parietalen und okzipitalen Bereichen. Entsprechende Unterschiede konnten auch durch Loreta-Lösungen bestätigt werden.

Unsere Daten zeigen, dass neben der bekannten FRN durch Feedback weitere Komponenten ausgelöst werden, die auch durch das Lernen mathematischer Regeln beeinflusst werden.

Investigation of NIRS-neurofeedback as a treatment method in adult ADHD: some preliminary data B. Barth, A.-C. Ehlis, U. Strehl, A.J. Fallgatter, K. Mayer, S. Wyckoff *Psychophysiologie und optische Bildgebung, Klinik für Psychiatrie und Psychotherapie, Tübingen*

Attention–deficit/hyperactivity disorder (ADHD) is one of the most common disorders of childhood. For a high proportion of cases, the primary symptoms – including inattentiveness, impulsivity, and hyperactivity – persist into adulthood. The estimated prevalence of clinician-assessed adult ADHD in the general population is 4-5 %. Impairments in educational, occupational, neuropsychological and social functioning are observed. Psychiatric comorbidities are highly prevalent in the adult ADHD population and include mood, anxiety, and substance abuse disorders. On a functional level, a dysfunction of the prefrontal cortex (PFC) has been assumed to underlie many of the deficits observed in ADHD. The present study is part of a larger project designed to compare the efficacy of specific biofeedback methods and protocols in changing core symptoms

as well as cognitive and neurophysiological variables in adult ADHD patients. Our purpose in the present study is to evaluate the feasibility of conducting a trial of near-infrared spectroscopy (NIRS)-neurofeedback for the treatment of adult ADHD patients. In neurofeedback training, self-regulation of specific aspects of brain activity can be learned via contiguous feedback and positive reinforcement. In NIRS-neurofeedback up-regulation of activity in the prefrontal cortex is operationalized as an increase in the concentration of oxygenated hemoglobin (O2Hb) within a predefined region of interest (NIRS channels covering left and right lateral prefrontal areas). During the deactivation period, on the other hand, subjects should achieve a decrease in O2Hb concentration within the same target region. We will present preliminary data of 10 adult patients diagnosed with ADHD (combined, hyperactive, or inattentive type) assessing whether they are able to learn cortical self-regulation with NIRS-neurofeedback. Further, changes in neurocognitive functions related to the treatment will be reported.

Unterschiede im EEG zwischen engem und weitem Aufmerksamkeitsfokus in einem simulierten Sportsetting M. Doppelmayr (1), E. Weber (2), N. Pixa (1), T. Möckel (2), K. Hödlmoser (2) *(1) Institut für Sportwissenschaft, Universität Mainz, Deutschland (2) Institut für Psychologie, Universität Salzburg, Österreich*

In Hinblick auf die psychologischen Aspekte sportlicher Aktivität stellt die Aufmerksamkeit eine grundlegend wichtige Komponente dar. Vor allem, aber nicht nur, in Mannschaftssportarten ist es wichtig, den Aufmerksamkeitsfokus entsprechend der jeweiligen Spielsituation zu wählen und ausrichten zu können. Um die biopsychologischen Parameter die einer solchen Veränderung des Aufmerksamkeitsfokus zugrunde liegen zu untersuchen, wurden Versuchspersonen (Vpn) gebeten als Reaktion auf einen Hinweisreiz die visuelle Aufmerksamkeit entsprechend zu variieren. Dazu wurden auf einem Monitor sieben Spieler in Form von schwarz/weiß Zeichnungen dargestellt von denen einer oder keiner einen Ball in den Händen hatte.

Abhängig vom Hinweisreiz (–2000 ms) sollten die Vpn beurteilen, ob der Spieler in der Mitte (enger Aufmerksamkeitsfokus) oder irgendeiner der dargestellten Spieler (weiter Aufmerksamkeitsfokus) den Ball hatte. Im Hinblick auf die Aufmerksamkeitszuwendung waren Unterschiede zwischen engem und weitem Fokus einerseits für das Zeitintervall zwischen Hinweis und Bild (–2000 bis 0 ms Prestimulus) und andererseits direkt nach der Stimuluspräsentation zu erwarten. Die Daten von 28 rechtshändigen Versuchspersonen konnten analysiert werden.

Im Prestimulusintervall wurde für 3 Zeitfenster von jeweils 500 ms (–1500 bis –1000, –1000 bis –500 und –500 bis Stimulusonset) die Event-related Desynchronization (ERD) des μ-Rhythmus (10 bis 13 Hz) berechnet und zwischen den Gehirnarealen der linken und der rechten Hand (C3 vs C4) verglichen. Hier zeigte sich ein signifikanter Unterschied im zeitlichen Verlauf der μ-ERD dahingehend, dass bei engem Fokus das Ausmaß der ERD auf C3 stärker ausgeprägt war.

Für den Zeitraum nach der Stimuluspräsentation wurden Event-related Potentials (ERPs) berechnet und eine späte, positive Komponente bestimmt (LPC). Der Vergleich der Amplituden der Midline Elektrodenpositionen (Fz, Cz, Pz und Oz) zeigte signifikante Unterschiede zwischen engem und weitem Aufmerksamkeitsfokus sowie zwischen einfachen (Ball in der Mitte) und

schwierigeren Aufgaben (Ball in der Peripherie oder kein Ball).

Individuality matters – emerging and persisting "neo-phrenologic" argumentation in the neurosciences bears the risk of oversimplifying models on the neural organisation of complex cognition and emotion T. Fehr *Center for Advanced Imaging, Center for Cognitive Sciences, Dpt. Neuro-psychology, University of Bremen, Germany*

Usually based on lesion studies, modular models on the neural organisation of complex mental processing tend to assume that there are rather closely spaced sections of brain tissue, which provide a sufficient neural basis for the mental processing of specific complex cognitions and emotions. Network-oriented theories, on the other hand, favour models, in which multiple parts of the brain or nested neural networks provide an adaptive neural substrate of complex mental processing. Indeed, growing evidence from the neurosciences confirm individual brain activation characteristics, potentially modulated by more or less consistent appliance of individual mental strategies acquired during individual lifelong learning histories and triggered by specific situation-related environmental requirements. Furthermore, the complexity of oscillatory network communication codes also appear to contribute to differences in individual brain activation properties. Analogous to the cognit-model introduced by Joaquin A. Fuster (e.g., 2006), a neuro-developmental model for the neural organisation of complex mental processing is described here. It is assumed that neural developmental starting regions that are assumed to work according to general complex mental principles (canonical perceptual, manipulating, integrating) can be localised in a modular way, for example, in the hetero-modal association cortices (e.g., intraparietal, middle frontal, medial frontal). Starting in these putatively genetically pre-defined regions from the outset of brain-maturing, cognitive development consecutively triggers neural sprouting and networking towards adjacent hetero-modal association cortices based on individual experiences and learning histories (Fehr, 2013). It might be the case that what is localised with neuroscientific approaches represents not the WHAT, but rather the HOW specific complex cognitions are organised and processed in the individual brain. Furthermore, sufficient individual features might be neglected by group-statistical approaches and so-called regions of interest analyses.

Neural Aspects of Inter-Individual Differences in Chronic Shopping Orientation S. Hügelschäfer (1), A. Achtziger (2), A. Florack (3), A. Jaudas (4), T. Fehr (5) *(1) Department of Economics, University of Cologne Hanse-Wissenschaftskolleg, Delmenhorst (2) Chair of Social and Economic Psychology, Zeppelin University Friedrichshafen (3) Department of Applied Psychology: Work, Education, Economy, University of Vienna (4) Chair of Social and Economic Psychology, Zeppelin University Friedrichshafen (5) Center for Advanced Imaging, Universities of Bremen and Magdeburg Center for Cognitive Sciences, University of Bremen*

We investigated how a consumer's chronic shopping orientation (utilitarian vs. hedonic, questionnaire-based measure) is reflected in the spatio-temporal dynamics of neural activity associated with the processing of shopping-related stimuli.

Participants were 19 female students whose EEGs were recorded while they passively viewed shopping-related pictures (scenes from different types of stores and shopping malls) and pleasant,

unpleasant, and neutral pictures taken from the IAPS.

For each contrast between different stimulus categories, a multiple source model was fitted based on the grand-average difference ERPs. Next, we applied these group-related models to the difference ERPs of each individual participant. This resulted in high residual variances, implying a large amount of inter-individual heterogeneity in spatial neural generator distributions. Therefore, we expanded each individual model by fitting additional individual sources until a saturated model was achieved.

Results showed that the more hedonic a participant's shopping orientation, the more additional individual frontal sources were necessary to sufficiently explain the difference between the spatio-temporal neural processing of shopping-related vs. neutral pictures. This finding indicates that a larger hedonic orientation might be associated with a more complex and regionally distributed and/or more idiosyncratically organized action-related or conceptual elaboration of shopping-related stimuli in frontal brain areas. Furthermore, we found significant correlations between the strength of neural activity of the group-related sources and participants' shopping orientation, which were interpreted as follows: In rather utilitarian participants there seems to be a very early distinction between shopping-related and neutral pictures, which might reflect an immediate frontal inhibition/blocking of potential effects of shopping-related picture cues. In contrast, more hedonic participants seem to exhibit a late perceptual in-depth analysis of these stimuli in the occipital cortex.

Our findings indicate that the neural elaboration of shopping as a hedonic experience appears to be organized highly idiosyncratically, which points to the relevance of a person's individual learning history.

Common cortical functional connectivities in a 3-center EEG study of acute first episode schizophrenia before treatment

D. Lehmann (1), P.L. Faber (1), R.D. Pascual-Marqui(1), R Achermann (1), P. Milz (1), M. Koukkou (1,2), W.M. Herrmann†(3), G. Winterer (3), N. Saito (4), K. Kochi (1) *(1) The KEY Institute for Brain-Mind Research, Department of Psychiatry, Psychotherapy and Psychosomatics, University Hospital of Psychiatry, Zurich, Switzerland (2) University Hospital of Psychiatry, University of Bern, Switzerland (3) Laboratory of Clinical Psychophysiology, Dept. of Psychiatry, University Hospital Benjamin Franklin, Free University of Berlin, Germany (4) Dept. of Neuropsychiatry, Kansai Medical University, Moriguchi, Osaka, Japan*

The concept of dissociation has been used to describe the brain mechanism of schizophrenia, implying a deteriorated functional connectivity between brain areas. Reported increased EEG dimensional complexity and decreased fMRI functional connectivity support this concept. We investigated whether EEG data from different centers support this conceptualization as common result across centers. Data of acute first episode schizophrenics before treatment were available from three university hospitals of psychiatry ($N =$ patients,controls: Bern $N = 9,36$; Berlin $N = 12,12$; Osaka $N = 9,9$) covering the six frequency bands of delta through beta2. Standardized low resolution electromagnetic tomography (sLORETA2008) was used to compute from the scalp EEG data the cortical sources at 19 cortical Regions-of-Interest, the physiological connectivities between them (excluding zero phase lag results possibly due to volume conduction), and

the t-test differences of the 171 connectivities between patients and controls for each frequency band and center. Conjunction analysis combined the results across centers, determining those qualifying significant connectivities that were common for the three centers. Of all 1026 connectivities (171 for each of the 6 frequency bands), at $p < 0.01$ (not corrected for multiple testing), 38 connectivities were decreased in the patients (6 in theta, 26 in alpha1, 3 each in beta1 and beta2), and 13 were increased in the patients (9 in delta, 1 in alpha2, 1 in beta1 and 2 in beta2); the delta-band increases were more to the right than the alpha1 decreases ($p = 0.09$). At $p < 0.001$, there were 4 decreased connectivities in the routine processing EEG frequency alpha1, and 2 increases in the processing-inhibiting EEG frequency of delta. As the majority of significant changes at $p < 0.01$ (41/51) concerned decreases of connectivity in the routine processing EEG frequencies of theta and alpha1 and increases in the processing-inhibiting EEG frequency of delta across three independent studies, the present results strongly support the concept of dissociation in schizophrenia.

Verbalizing or visualizing thoughts correlates with hemispheric amplitude and latency of checkerboard ERP P. Milz, P.L. Faber, K. Kochi, D. Lehmann *The KEY Institute for Brain-Mind Research, Department of Psychiatry, Psychotherapy and Psychosomatics, University Hospital of Psychiatry, Zurich, Switzerland*

Persons differ in their thinking style: In words (verbalization) or in schematic images (spatial visualization) or in realistic images (object visualization). Speech processing in right-handers is in the left hemisphere, visual processing predominantly in the right hemisphere. We did a pilot study to test the hypothesis that a meaningless visual stimulus (checkerboard reversal) reflects the hemispheric preference of the three thinking styles. 60 healthy, male, right-handed participants answered the „Modality of Thinking Questionnaire“ (self-rating in 3 scales: verbalization, spatial visualization, object visualization). Checkerboard reversal-event related responses (upper hemiretina, 2/s, 1.5-20 Hz, 64 channels, 2048 samples/s) were averaged in three channels (F3 and P3: speech hemisphere; P4: visual hemisphere) versus 64-channel average reference. During 80-115 ms post-stimulus, latency and amplitude at the amplitude trough of F3 and at the amplitude peaks of P3 and P4 were determined. The three self-ratings were correlated (Pearson) with the latencies and amplitudes. Agreeing with the hypothesis (1-tailed p-values), higher verbalization ratings correlated with shorter latencies over the left hemisphere (F3: $r = -0.199, p = 0.07, N = 55$; P3: $r = -0.293, p = 0.02, N = 49$), and higher spatial visualization ratings as well as higher object visualization ratings correlated with greater amplitudes over the right hemisphere (P4: $r = 0.204, p = 0.08, N = 51$, and P4: $r = 0.223, p < 0.06, N = 51$, respectively). We conclude that preferred modalities of thinking are associated with speed and intensity of neuronal activation: the left hemisphere reflects verbalizing tendency by shorter evoked latencies; the right hemisphere reflects visualizing tendency by greater evoked amplitudes. One could assume that tending to verbalize thoughts leads to more engaged left hemispheric processing, while tending to visualize thoughts to more engaged right hemispheric processing. Alternatively, inherited superior processing capabilities of certain areas might lead to preferentially thinking in the corresponding modalities.

The emotional prosody of mismatch negativity (MMN) in schizophrenic patients and healthy controls C. Norra, H. Thönneßen, E. Köhler, J. Ostermann *Klinik für Psychiatrie, Psychotherapie und Präventivmedizin, Labor für Klinische Neurophysiologie, LWL-Universitätsklinikum, Ruhr-Universität Bochum, Deutschland*

Institut für Neurowissenschaften und Medizin, Physik der Medizinischen Bildgebung, Forschungszentrum Jülich, Deutschland

Die Mismatch Negativität (MMN) wird als Subtraktionswelle akustischer ereigniskorrelierter Potentiale generiert, wenn in der vorbewussten, kortikalen Informationsverarbeitung abweichende Stimuli prozessiert werden. Insbesondere schizophrene Patienten weisen eine verminderte MMN auf. Dies gilt auch für die neuartigen optimierten MMN-Paradigmen mit multiplen abweichenden Stimuli (Näätänen et al. 2004), wo wir ein solches Defizit auch bei schizophrenen Patienten demonstrieren konnten (Thönneßen et al. 2008). Die Weiterentwicklung dieser kognitiven Paradigmen mit prosodischen Stimuli ermöglicht auch, den frühen kortikalen Einfluss emotionaler Komponenten auf die MMN-Informationsverarbeitung zu untersuchen (Thönneßen et al. 2010). In dieser Studie sollen nun schizophrene Patienten, die neben produktiven Symptomen wie Wahn und Sinnestäuschungen mittel- und langfristig vor allem durch ihre Negativsymptomatik wie der affektiven Verflachung beeinträchtigt, untersucht werden.

21 stationäre schizophrene Patienten (ICD-10: F20.x) und 21 gesunde Probanden wurden unter Ableitung eines Multikanal-EEG mit traditionellen („oddball“) und optimierten akustischen MMN-Paradigmen, basierend auf emotionalen Pseudowörtern, untersucht. Die Pseudowörter entstammen dem Magdeburger Prosodie-Korpus und wurden in unterschiedlicher emotionaler Prosodie (neutral, fröhlich, wütend, traurig) sowie einem geschlechtsalternierenden Sprecher eingespielt. Psychometrische Daten wurden mit Selbst- und Fremdbeurteilungsinstrumenten (Beck Depressions Inventar BDI, Brief Symptom Inventary BSI, Positiv und Negative Syndrom Skala PANSS) erhoben

Bei schizophrenen Patienten wurde, am deutlichsten im optimierten MMN Paradigma, eine geringere prosodische MMN bei fröhlichen und traurigen Pseudowörtern gegenüber den gesunden Kontrollen beobachtet, jedoch nicht auch für die Kategorie Wut. Die Ergebnisse blieben auch nach Betrachtung der Effekte von Alter und Geschlecht signifikant. Für verschiedene psychometrische Variablen fanden sich negative Korrelationen mit der MMN in der Gruppe der Patienten, hier vornehmlich in Korrelation zum Oddball-Paradigma, und unabhängig von der emotionalen Valenz.

Erstmals konnte gezeigt werden, dass die frühe kortikale Informationsverarbeitung der prosodischen MMN bei schizophrenen Patienten beeinträchtigt ist. Zusammenfassend erweist sich die emotionale prosodische MMN als ein wertvolles Werkzeug für die Untersuchung der basalen emotionalen Informationsverarbeitung.

Exploring effective connectivity by a Granger Causality approach with embedded dimension reduction B. Pester, L. Leistritz, H. Witte, A. Wismueller *Universitätsklinikum der Friedrich-Schiller Universität Jena*

A basic problem in quantifying directed information transfer is the consideration of effective connectivity in very high-dimensional (HD) systems. Currently, HD systems are transformed into lower dimensional systems, e.g. by Principal or Inde-

pendent Component Analysis (PCA, ICA), and the connectivity structure of derived components is studied. The drawback is that discovered interactions cannot be readily transferred back into the original HD space. Thus, directed interactions between the original network nodes are not revealed, which limits the interpretability of identified interaction patterns.

Granger Causality (GC) is a suitable concept for assessing connectivity structures between time series. One popular approach uses principles of prediction, whereby application of a straightforward generalization to general time series models is enabled, providing an appropriate definition of prediction errors.

The basic idea of a large scale GC (lsGC) is the integration of a dimension reduction into a multivariate time series model, which allows computation of prediction errors in the original HD space. Instead of analyzing interactions between derived components, this approach preserves the interpretability of the original network nodes.

In order to provide a proof-of-principle we compared the lsGC approach with the conventional GC. Simulations using 50-dimensional multivariate autoregressive processes of various data lengths were analyzed. They consisted of five macro networks with 20 micro networks each. As resulting lsGC values yield high sensitivity and specifity for an adequate number of samples, the lsGC approach turned out to be appropriate to quantify directed information transfer in HD systems. Furthermore we tested the method on the basis of resting state fMRI data. We were able to show that even for a small number of retained components (3%), reasonable connectivity structures emerged.

In conclusion, lsGC is appropriate to extend the conventional GC concept to HD data and is worth to be applied to further analyses.

State Empathy affects the cortical processing of bodily emotion expressions – A functional near-infrared spectroscopy study S. Schneider (1), L. Tuchscherer (1), F.B. Häußinger (1), A. Christensen (2), M.A. Giese (2), A. Fallgatter (1), A.-C. Ehlis (1) *(1) Universitätsklinik für Psychiatrie und Psychotherapie Tübingen (2) Hertie Institut für Klinische Hirnforschung Tübingen*

The ability to recognize and adequately interpret emotional states in others plays an essential role in regulating social interaction and respective deficits frequently occur in individuals with psychological diseases. Although body language represents an essential element of nonverbal communication which is often perceived prior to mimic expression, most studies investigating emotion perception so far used static face stimuli. In recent experiments, however, body-selective brain areas have been increasingly focussed and some of these areas have been shown to be sensitive to bodily emotion expressions (e.g., fusiform gyrus [FG], extrastriate body area [EBA], superior temporal sulcus [STS], temporo-parietal junction [TPJ]). In a recent study, we were able to replicate enhanced activity within these areas when emotional vs. neutral gait patterns had been observed using functional near-infrared spectroscopy (fNIRS). Preliminary results further suggest altered brain activity in psychiatric patients while viewing emotional body language. However, so far very little is known about the potential involvement of frontal brain areas, e.g. the inferior frontal cortex, in these processes and it is unclear whether this automatic body-based emotion processing can be influenced by manipulations of

state empathy. In the present study, 40 healthy subjects were investigated using fNIRS while performing an emotion discrimination paradigm in which dynamic body expressions were presented in terms of walking avatars. Half of the subjects (empathy group) received holistic background information on the videos to enhance their situational empathy for the avatars, while the other 20 participants did not get any additional information (control group). fNIRS data analyses revealed brain activation increases within the prefrontal cortex (PFC) during the perception of emotional gait only in the empathy group, but not in the control group. These results suggest that the neural perception of body-based emotions can be affected by the observer's current empathy level.

Adult-like perception of prosodic boundary cues in six-month-old infants I. Wartenburger, J. Holzgrefe, C. Wellmann, B. Höhle *Linguistik, Universität Potsdam*

Säuglinge im Alter von 6 Monaten reagieren spezifisch auf prosodische Phrasengrenzen wie zum Beispiel Intonationsphrasengrenzen (intonation phrase boundaries, IPBs) (Seidl, JML, 2007). IPBs sind durch drei akustische Markierungen gekennzeichnet: Veränderung der Tonhöhe (pitch change), Dehnung (final lengthening) und eine Pause. Diese prosodischen Markierungen sind in verschiedenen Sprachen unterschiedlich gewichtet und die Sensitivität hierfür entwickelt sich im ersten Lebensjahr (Johnson & Seidl, Infancy, 2008; Seidl & Cristià, Dev.Sci, 2008; Wellmann et al., FrontPsych, 2012). In Reaktion auf die Wahrnehmung einer IPB zeigt sich im ereignis-korrelierten Potential (EKP) eine breite Positivierung (closure positive shift, CPS; Steinhauer et al., NatNeurosci, 1999). Unklar ist, ob sich ein CPS auch bei Säuglingen nachweisen lässt (siehe Pannekamp et al., NeuroReport, 2006 vs. Männel & Friederici, JCN, 2009) und ob Säuglinge ähnlich wie Erwachsene auf diese Markierungen reagieren. Um die Rolle der verschiedenen prosodischen Markierungen für die Entwicklung der Wahrnehmung prosodischer Phrasengrenzen zu charakterisieren, wurden bei 6-monatigen Säuglingen EKPs abgeleitet während sie kurzen Listen aus 3 Namen zuhörten. Dabei wurden pitch change sowie pitch change in Kombination mit final lengthening auf dem zweiten Namen manipuliert. Es zeigte sich, dass ein CPS elizitiert wurde, wenn pitch change und final lengthening als prosodische Grenzmarkierungen in den Stimuli vorhanden waren, nicht jedoch wenn nur pitch change vorhanden war. Dies entspricht den Ergebnissen Erwachsener und den Verhaltensdaten von 8-monatigen Säuglingen, die mittels headturn preference procedure erhoben wurden (Wellmann et al., FrontPsych, 2012). Die Daten weisen darauf hin, dass bei 6-monatigen Säuglingen nur eine Kombination von Tonhöhenveränderung und finaler Dehnung die Wahrnehmung einer IPB auslöst. Die Ergebnisse können nicht auf die Wahrnehmung der Pause bzw. obligatorische Onset-Komponenten zurückgeführt werden (Männel & Friederici, JCN, 2009), weil die Stimuli keine Pause enthielten. Da die Ergebnisse mit denen Erwachsener übereinstimmen, schlussfolgern wir, dass bereits 6-monatige Säuglinge prosodische Grenzen in einer erwachsenenähnlichen Art und Weise verarbeiten. Funding: DFG SPP 1234 (FR 2865/2-1; HO 1960/13-1)

Segmentation of IDS and ADS in 12-month-olds: An ERP study K. Von Holzen, D. Wolff, N. Mani *Junior Research Group "Language Acquisition", Göttingen, Deutschland*

To build up a vocabulary, the infant must extract, or segment, individual words from the language being spoken around them. Research has shown that at 7.5-months-of-age, infants are able to segment words from sentences (Jusczyk & Aslin, 1995) presented in infant-directed speech (IDS). However, only 15% of the speech in the infants'

environment is infant-directed (van der Weijer, 2002). At what age, then, do infants begin to segment words from "normal" or adult-directed speech (ADS)?

The current study tested German 12-month-olds on their ability to segment both IDS and ADS. Infants were presented with 40 familiarization-test blocks, half in IDS and the other half in ADS. In the familiarization phase, infants heard eight sentences, each containing the same (familiarized) word. In the test phase, infants heard the familiarized word and an unfamiliar control word. ERPs time-locked to the onset of the words in the test phase were examined for differences between familiarized and control words in IDS and ADS blocks. If infants extract the phonological form of the familiarized word from the sentences, recognition of this word-form should be indicated by more negative ERPs for familiarized compared to control words.

As predicted ERPs were more negative following familiarized compared to control words, 200-350ms after word onset in the test phase: infants successfully segmented the familiarized words from the sentences and recognized these words later in the test phase. The effect for IDS was greater than ADS; however, this difference was not significant. In summary, the current study demonstrates that German infants, as young as 12-months-of-age, are able to segment words from both ADS and IDS. This may provide further support to infants' ability to begin producing words by 12-months of age and their rapid vocabulary development later in the second year of life (Bloom, 1973).

Adjusting the processing of word stress and phonemes in the first year of life A.B.C. Becker (1), U. Schild (2), C.K. Friedrich (2) *(1) Biological Psychology and Neuropsychology, University of Hamburg, Germany (2) Developmental Psychology, University of Tübingen, Germany*

Language-specific learning for word-level stress has been shown in very young infants. It occurs even before infants figure out the typical phonemes (at least the typical consonants) of the maternal language. This suggests some independency between the processing of syllable-relevant information at the one hand and phoneme-relevant information on the other during infancy. Here we tested this assumption by means of Event-Related Potentials (ERPs) recorded in unimodal auditory word onset priming.

Spoken word onset syllables (primes) preceded spoken words (targets). We varied phoneme and stress overlap between primes and targets in four conditions: (i) "phoneme-match, stress-match" (e.g., MA - MAma, Engl. mummy [capitals indicate stressed syllables]); (ii) „phoneme-match, stress-mismatch" (e.g., ma- MAma); (iii) "phoneme-mismatch, stress-match" (e.g., SO-MAma); (iv) „phoneme-mismatch, stress-mismatch" (e.g., so-MAma).

ERPs of thirty 3-month-olds, thirty 6-month-olds and thirty 9-month-olds from German speaking environments were recorded. An early phoneme match effect, starting at around 100 ms after target onset, was present for all infant groups. A stress match effect, starting at around 300 ms, was present in the 3-month-olds and in the 9-month-olds. Phoneme and stress priming did not interact in both age groups. This suggests independent processing of both types of information in infancy. There was no stress match effect in the 6-month-olds. It appears that language processing is focused on phoneme-relevant information at that age.

Listen up! Learning of grammatical rules across infancy J.L. Mueller *Institut für Kognitionswissenschaften, Universität Osnabrück, Deutschland*

Auditory perception and language learning are closely intertwined. I will present a series of developmental event-related potential studies in which we explored whether and how pitch perception may impact on the ability to extract non-adjacent dependencies between syllables from the speech stream. Participants listened to frequent standard stimuli, which were interspersed with infrequent pitch deviants and rule deviants, violating a non-adjacent dependency between two syllables. In 3-month-old infants the mismatch response to rule deviants was linked to the mismatch response for pitch deviants. Concordantly, both mismatch effects were linked in adults who showed behavioral evidence of rule learning, however, under different task conditions. Further evidence from 2 and 4-year old children and its implication for specifying a developmental trajectory of linguistic rule learning from mere exposure will be discussed. The results point towards a role for basic perceptual processes during linguistic rule learning which changes across ontogenetic development.

The Impact of Different Language Learning Settings on the Processing of Phonotactic Properties in 6-Month-Old Infants - which Training Works Best? M. Richter (1,2), M. Vignotto (1,2), H. Obrig (1,2), S. Rossi (1,2) *(1) Day Clinic for Cognitive Neurology, Medical Faculty, University of Leipzig, Germany (2) Max Planck Institute for Human Cognitive and Brain Sciences, Department of Neurology, Leipzig, Germany*

Infants start establishing knowledge about the phonotactic rules of their native language already around 3 months of age. Phonotactics describes the possible arrangements of phonemes in a certain language. Acquiring this knowledge helps babies to segment the incoming auditory speech stream as phonotactic properties signal word boundaries.

In our study we investigate how neuronal responses to native (i.e., legal) and non-native (i.e., illegal) phonotactic regularities are modulated by two different language learning settings in 6-month-old infants.

Each infant underwent a pretest, a training (passive listening training or semantic training), and a posttest on three consecutive days. Pretest and posttest included acoustically presented pseudowords, which were either phonotactically legal or illegal. The passive listening training consisted of the pure acoustic presentation of pseudowords. During the semantic training the pseudowords were combined with pictures of real objects creating an associative learning setting. Brain activity responses were monitored by means of event-related brain potentials (ERPs). Preliminary ERP results indicate a familiarization effect for phonotactically legal and illegal trained pseudowords. The familiarization was indexed by increasing deflections in posterior brain regions, displayed from day 1 to day 3. The deflections were larger for legal than for illegal trained pseudowords and were not present for untrained pseudowords. Brain activity modulations were more prominent in infants undergoing the semantic training than in babies belonging to the passive listening group.

These findings reveal that word learning mechanisms emerge very early in life eliciting changes in the brain. The familiarization effect points to acoustically oriented perceptual mechanisms guiding word learning at this early age. The results suggest that the kind of learning scenario impacts brain modulations differently in 6-month-old infants. The semantic learning context might

display a more natural and attracting language learning context than passive listening thus eliciting larger brain plasticity effects in comparison to passive listening.

The prerequisites for language development: speech-relevant auditory discrimination of deaf children following early cochlear implantation N. Vavatzanidis (1,2), D. Mürbe (2), A. Hahne (2) *(1) Max-Planck-Institut für Kognitions- und Neurowissenschaften, Leipzig (2) Sächsisches Cochlear Implant Centrum, HNO, Universitätsklinikum Dresden*

Im Fokus dieser Studie stand die Frage, was kongenital stark hörgeschädigte Kinder, die erst mit Hilfe eines Cochlea-Implantats (CI) Zugang zu akustischem Input bekommen, in den ersten Monaten an sprachrelevanten Merkmalen wahrnehmen. Auditorische Diskriminierungsfähigkeiten, wie die Unterscheidung variierender Silbenlänge, sind elementare Voraussetzungen für den kindlichen Spracherwerb.

Durch elektrophysiologische Studien ist bekannt, dass normalhörende Kinder im Alter von zwei Monaten unterschiedliche Silbenlängen differenzieren können. In der Studie sollte untersucht werden, ob sich bei kongenital stark hörgeschädigten Kindern, die bis zum vierten Lebensjahr mit einem CI versorgt wurden, diese Unterscheidungsfähigkeit in einem ähnlichen Zeitrahmen entwickelt oder ob der späte Onset der ersten auditorischen Stimulation die Entwicklung und somit die Voraussetzungen für den Spracherwerb verzögert. Das Elektroenzephalogramm von 14 kongenital ertaubten Kindern (mittleres Alter bei Implantation: 1,7 Jahre) wurde in der Woche der Erstanpassung des Implantats sowie nach jeweils zwei, vier und sechs Monaten gemessen. In einem klassischen Oddball-Paradigma wurde den Kindern eine Silbe mit zwei unterschiedlichen Vokallängen präsentiert.

Im Ergebnis zeigt sich, dass zum Zeitpunkt der Erstaktivierung des Implantats noch keine Unterscheidung der unterschiedlich langen Silben zu erkennen ist. Ab zwei Monaten Tragedauer zeichnet sich ein Unterscheidungseffekt in Form einer Mismatch Negativity im Zeitfenster von 200 bis 300 ms deskriptiv ab. Dieser Effekt wird ab vier Monaten Tragedauer beim Kontrast von devianten langen Silben mit kurzen Standardsilben signifikant ($p < 0.001$). Das Unterscheiden verschiedener Silbenlängen scheint demnach wenige Tage nach Erstanpassung des Implantats noch nicht möglich zu sein, sondern erfordert eine Hörgewöhnung von bis zu vier Monaten.

In Hinsicht auf die lange Phase von Geburt bis Implantation ohne sprachrelevante auditorische Stimulation holen die in jungem Alter implantierten Kinder im Vergleich zu normalhörenden Kindern jedoch schnell auf und erschließen sich somit das Fundament für den weiteren Spracherwerb.

ERPs as a marker of language comprehension in adult cochlear implant patients A. Hahne, D. Mürbe *Sächsisches Cochlear Implant Centrum, HNO, Universitätsklinikum Dresden*

Das Cochlea-Implantat (CI) ist eine Neuroprothese, die die Funktion der Hörschnecke ersetzt. Postlingual ertaubte Erwachsene können in der Regel mit einem CI gut rehabilitiert werden, wenngleich es deutliche interindividuelle Differenzen gibt. In jedem Fall aber erfordert das Sprachverstehen mit CI zunächst einen Lernprozess, da die resultierenden sprachlichen Wahrnehmungen nicht mit den im Gehirn gespeicherten Repräsentationen übereinstimmen. Die vorliegende Studie untersucht diese Lernprozesse mittels evozierter Potentiale auf akustisch präsen-

tierte Wörter. 11 CI-versorgte Erwachsene mit beidseitiger, postlingualer Hörschädigung nahmen an dem Experiment teil.

In den ersten vier Tagen nach Aktivierung des Sprachprozessors sowie nach weiteren 2 Monaten wurden bei allen Patienten EEG-Messungen durchgeführt. Es wurden Wörter präsentiert, die von Bildinformationen begleitet wurden, die entweder einer korrekten Bezeichnung des dargestellten Gegenstandes entsprachen oder nicht. Nach einer Lernphase wurden dieselben Bild-Wortpaarungen erneut präsentiert, gepaart mit neuen Bild-Wortkombinationen. Anschließend wurden akustisch evozierte Potentiale auf den Wortstimulus gemittelt.

Bereits in den ersten Tagen nach Erstanpassung konnte ein Kongruenzeffekt im EKP beobachtet werden. Dieser Effekt trat jedoch im Vergleich zu klassischen N400-Effekten sehr spät auf ($\approx$ ab 800 ms nach Wortonset). Im Anschluß an eine Lernphase war die Latenz des Effektes jedoch bereits um etwa 200 ms reduziert. Für zuvor nicht gehörte Wörter war der Kongruenzeffekt deutlich schwächer ausgeprägt.

Nach 2 Monaten CI-Tragedauer hatten sich alle Kongruenzeffekte deutlich stabilisiert und zeigten frühere Onsetlatenzen und größere Amplituden, wenngleich die Latenzen noch nicht mit denen Normalhörender vergleichbar waren.

Die Daten quantifizieren den sprachlichen Adaptations- und Lernprozess bei postlingual ertaubten CI-Patienten. Während das Sprachverarbeitungssystem zu Beginn der Prozessoraktivierung noch erheblich mehr Zeit für ein Matching von gehörter Information und gespeicherter Repräsentation der Wörter benötigt, nimmt diese Verarbeitungszeit mit zunehmender Tragedauer ab.

Announcements — Ankündigungen

- **IOP World Congress**

  The 17th World Congress of Psychophysiology (IOP2014) will take place in Hiroshima, Japan from September 23 to 27, 2014.

  Information and Registration at: http://www.iop2014.jp/

- **23. Deutsches EEG/EP Mapping Meeting / 23rd German EEG/EP Mapping Meeting**

  Conference language is German; English contributions will be accepted.

- Workshops
  - M. Kottlow, Th. Koenig (Bern), Resting state and state dependent information processing in health and disease, Symposium.
  - A. Mierau (Köln), Neuromechanik und Neuroplastizität im Sport, Symposium.
  - C. Wolters (Münster), S. Rampp (Erlangen), EEG, MEG and combined EEG/MEG source analysis in presurgical epilepsy diagnosis, Workshop.
- 24. bis 26. Oktober 2014; Schloss Rauischholzhausen
- Anmeldeschluss ist der 15. Juli 2014.
- Information und Anmeldung unter: http://www.med.uni-giessen.de/physio/